



Minimal dissipation protocols of an instantaneous equilibrium Brownian particle under time-dependent temperature and potential variations

Yonggun Jun (전용근) * and Pik-Yin Lai (黎璧賢) †

Department of Physics and Center for Complex Systems, National Central University, 300 Zhong-Da Road, Taoyuan City, Taiwan 320, Republic of China



(Received 28 February 2022; accepted 16 May 2022; published 27 May 2022)

We consider the instantaneous equilibrium (ieq) transition of an underdamped Brownian particle under arbitrary time-dependent temperature and potential variations and derive analytic results for the temperature and potential protocols for minimal dissipative work. Explicit results for the time-dependent minimal dissipation protocols and the associated energetics are obtained for the cases of pure temperature variation, pure potential parameter (stiffness) variation, and isentropic ieq processes. The minimal dissipation condition enforces the forward and backward protocols to be time-reversal related, with the same minimal dissipative work. Remarkably, it is shown that the minimal dissipation path is also the isentropic ieq transition. The energetics in the mdieq transitions are analyzed in detail with emphasis on the conditions for maximizing the mean work and power that can be extracted. Furthermore, exact results for the overdamped limit are derived, indicating that there is great freedom to choose the minimal dissipation protocols, thus allowing the realization of mdieq transitions in Brownian colloidal systems with relative ease.

DOI: [10.1103/PhysRevResearch.4.023157](https://doi.org/10.1103/PhysRevResearch.4.023157)

I. INTRODUCTION

The last three decades marked the breakthrough in the understanding of nonequilibrium statistical physics, especially in the far from equilibrium and fluctuation dominating regimes. New physical laws, such as fluctuation theorems [1,2] and theoretical techniques such as stochastic thermodynamics [3,4], proved to be very successful in a broad range of nonequilibrium processes in small systems in which thermal fluctuations dominate. These theories have been demonstrated to be quantitatively accurate in various experimental systems, such as colloidal systems [5–7], electric circuits [8–10], Brownian heat engines [11–13], biological systems [14,15], and quantum systems [16,17]. Due to the theoretical and experimental advances of the nonequilibrium physics in strongly fluctuating systems, we are ready for the applications of stochastic energetics in microscopic systems dominated by fluctuations, such as manipulating or designing transition paths with special properties. For example, it is possible to achieve a finite-rate transition between two designated equilibrium states [18–20] via a nonequilibrium path and to reduce the dissipated work [21]. The positive entropy production for a transition between two equilibrium states implies that the process is in general irreversible unless the transition path is

quasistatic, i.e., reversible and zero-entropy production process can only be achieved infinitely slow such that equilibrium is kept at every moment during the transition. Speeding up the transition from one equilibrium state to another in a time much shorter than the intrinsic relaxation time while reproducing the same output as a quasistatic process, has been a challenging issue, which requires nontrivial control protocols of one or more parameters [22].

Recently, the shortcut-to-isothermality protocol which can achieve a finite-rate isothermal transition while keeping the system in instantaneous equilibrium (ieq) at a fixed temperature during the transition was theoretically derived [23,24] and experimentally demonstrated for time-dependent variations on the parameter on a potential, such as having a time-dependent stiffness on the harmonic potential [25,26]. However, in many theoretical and practical situations, such as in the construction of microscopic heat engine cycles, one would like to heat up or cool down the system with some time-dependent temperature protocols. Very recently, we have derived the theoretical conditions for ieq under both time-dependent temperature and potential-parameter protocols for an underdamped Brownian particle [27]. The ieq recipe for time-varying potential and temperature under harmonic and nonharmonic trapping potentials were obtained and verified by Langevin dynamics simulations. Remarkably, it was demonstrated that it is possible to achieve ieq isentropic and zero entropy change processes, and the existence of work and heat relations for the ieq protocols of the forward and reverse processes was established [27].

With the powerful machineries developed due to the advances of stochastic thermodynamics, we are now in a stage to utilize these ideas and tools to construct more realistic microscopic heat engines for practical applications. This opens

*yonggun@phy.ncu.edu.tw

†pylai@phy.ncu.edu.tw

Published by the American Physical Society under the terms of the [Creative Commons Attribution 4.0 International license](https://creativecommons.org/licenses/by/4.0/). Further distribution of this work must maintain attribution to the author(s) and the published article's title, journal citation, and DOI.

up the possibilities of designing microscopic heat engines that can run in a much faster cycle time and better power extraction. Since fluctuations in microscales cannot be ignored, a deep understanding of their physical properties is vital to the working principles and enhancing the efficiencies of these micro heat engines. Several optimal protocols were proposed for the purpose of minimizing transition times [19,28–31] or dissipative work [21,32–35], in the context of given initial and final equilibrium distributions subjected to different constraints. The geometry and minimal energy path of shortcuts to isothermality and has also been recently studied [36]. To realize the finite-time heat engine [37] that can effectively extract useful work, appropriate independent control of temperature and potential is essential for constructing transition paths in engine cycles.

A major benefit of implementing ieq transitions is that the properties of the system is fully described by the Boltzmann distribution as if the system is at equilibrium, and yet the transition rate can be fast. With the full knowledge of the probabilistic description of the system, not only can one have deeper insights, it also opens the broad avenue of achieving better control of the system and implementing appropriate manipulations for designated purposes. In addition, the relevant stochastic energetics for ieq transitions can also be conveniently calculated. Equipped with the above mentioned advantage, it would enhance the possibility to design pathways with prescribed properties to overcome practical limitations and achieve optimal energetic performance.

In this paper, we develop the theory of achieving an ieq path with minimal dissipation for general underdamped systems under time-varying temperature and potential. Explicit protocols for minimal dissipation ieq (mdieq) under constant temperature, under a fixed potential, and under isentropic condition are derived. In practice, realizing underdamped stochastic systems with heating and cooling protocols are experimentally challenging. On the other hand, the experimental convenient Brownian colloidal system lies in the overdamped limit since the timescale related to inertial force is much smaller than the relaxation time of the trapped colloid. Hence, the overdamped limit for the mdieq transition is also considered in this paper, with more explicit analytic results derived that are applicable in the experimental implementation in colloidal systems.

II. IEQ PROTOCOL AND ENERGETICS FOR TIME-DEPENDENT POTENTIAL AND TEMPERATURE PROCESSES

As described in Ref. [27], we consider an underdamped Brownian particle of mass m and damping coefficient γ moving in one dimension under the potential $U_0(x, \lambda(t))$, where $\lambda(t)$ is the time-dependent protocol that drives the potential and τ is the duration of the transition. As pointed out in Refs. [12,27], underdamped dynamics is essential in correctly describing the stochastic dynamics and energetics for processes involving temperature changes, even in the overdamped limit. The time-dependent Hamiltonian of the single Brownian particle system is given by

$$H_0(x, p, \lambda(t)) = \frac{p^2}{2m} + U_0(x, \lambda(t)), \quad (1)$$

where p is the momentum of the particle. At the same time, the temperature of the system is also changing whose protocol is given by $T(t)$ or the inverse temperature $\beta(t) = 1/T(t)$ (the Boltzmann constant is set to unity for simplicity). To achieve instantaneous equilibrium (ieq), the ramp potential $U_0(x, \lambda(t))$ is escorted by a position and momentum-dependent auxiliary potential $U_1(x, p, t)$ [23,27] so that the particle experiences a total Hamiltonian

$$H = H_0(x, p, \lambda(t)) + U_1(x, p, t) \quad (2)$$

such that the underdamped Brownian particle will be in an ieq state obeying the Boltzmann distribution $\rho_{\text{ieq}}(x, p, t) = e^{\beta(t)(F(\lambda, \beta) - H_0(x, p, \lambda(t)))}$, where $F(\lambda, \beta) = -\frac{1}{\beta(t)} \ln \int dp \int dx e^{-\beta(t)H_0(x, p, \lambda(t))}$ is the free energy of the ramp system at ieq for some instantaneous value of λ and β . The auxiliary potential $U_1(x, p, t)$ can be determined for a given ramp potential $U_0(x, \lambda(t))$ with the protocols $\lambda(t)$ and $\beta(t)$ (see Appendix A for a summary). It can be shown [27] that the solution $U_1(x, p, t)$ can be put into the form

$$U_1(x, p, t) = \dot{\lambda}(t)f(x, p, \lambda(t), \beta(t)) + \dot{\beta}(t)g(x, p, \lambda(t), \beta(t)) \quad (3)$$

for some functions f and g , where $\dot{}$ denotes the derivative with respect to time. For a smooth switching on and off of the auxiliary potential, one usually imposes the boundary conditions $\dot{\lambda}(0) = \dot{\lambda}(\tau) = \dot{\beta}(0) = \dot{\beta}(\tau) = 0$, but these are not required for the derivation of U_1 . In this paper, we relax these B.C.s and consider transitions between the initial state $(\lambda(0), \beta(0))$ to the final state $(\lambda(\tau), \beta(\tau))$.

Under the ieq protocol, the Brownian particle will experience the potential $U_{\text{ieq}}(x, p, t) \equiv U_0(x, \lambda(t)) + U_1(x, p, t)$ and will be at ieq and obey the Boltzmann distribution $\rho_{\text{ieq}}(x, p, t)$ at any time ($0 \leq t \leq \tau$) during the transition process. In this paper, we focus on harmonic and nonharmonic trapping potentials of the form

$$U_0 = \frac{1}{2}\lambda(t)x^n, \quad n = 2, 4, 6, \dots \quad (4)$$

for analytic calculations.

One can write the potential protocol in terms of the dimensionless function $\Lambda(t)$ as $\lambda(t) = \lambda_0 \Lambda(t)$, where λ_0 is some fixed value of λ , and express all energy scales in terms of the some fixed inverse temperature β_0 . For U_0 of the form (4), one can express all lengths in terms of the natural spatial scale $\sigma \equiv (\beta_0 \lambda_0)^{-\frac{1}{n}}$, and express time in unit of the relaxation time $\tau_r \equiv \frac{\beta_0 \gamma}{(\beta_0 \lambda_0)^{2/n}}$. For underdamped dynamics, $\tau_m \equiv m/\gamma$ is the inertia memory timescale. The Hamiltonian and potentials can be written using the dimensionless space, time, and momentum ($\tilde{x} \equiv x/\sigma$, $\tilde{t} \equiv t/\tau_r$, $\tilde{p} \equiv p\tau_r/(m\sigma)$) variables. Hereafter, with the understanding that all space, time, and momentum variables are expressed in their dimensionless form, the superscript \sim will be dropped for notation convenience. In terms of these dimensionless variables, the time-dependent ramp potential is given by

$$\beta_0 U_0 = \frac{1}{2} \Lambda(t) x^n \quad (5)$$

and the auxiliary potential U_1 under time-dependent drivings of $\lambda(t)$ and $\beta(t)$ is given by [27] (see the summary in

Appendix A)

$$\beta_0 U_1 = \frac{v(t)}{2n} [(\alpha p - x)^2 + \alpha \Lambda(t) x^n] + \frac{\dot{\beta}(t)}{4\beta(t)} [(\alpha p)^2 + \alpha \Lambda(t) x^n] \quad (6)$$

$$\alpha \equiv \frac{\tau_m}{\tau_r}; \quad v(t) \equiv \frac{\dot{\Lambda}(t)}{\Lambda(t)} + \frac{\dot{\beta}(t)}{\beta(t)}. \quad (7)$$

Because of the ieq nature, the averages for various observables during the transition can be easily derived, for example,

$$\alpha \langle p^2(t) \rangle = \frac{\beta_0}{\beta(t)}, \quad \langle x^n(t) \rangle = \frac{2\beta_0}{n\beta(t)\Lambda(t)},$$

$$\langle x^2(t) \rangle = \left(\frac{2\beta_0}{\beta(t)\Lambda(t)} \right)^{\frac{2}{n}} \frac{\Gamma(\frac{3}{n})}{\Gamma(\frac{1}{n})}; \quad (8)$$

$$\langle U_0(t) \rangle = \frac{1}{n\beta(t)}, \quad (9)$$

$$\langle U_1(t) \rangle = \frac{\alpha}{\beta(t)} \left(\frac{1}{2} + \frac{1}{n} \right) \left(\frac{v(t)}{n} + \frac{\dot{\beta}(t)}{2\beta(t)} \right) + \frac{\Gamma(\frac{3}{n})}{\Gamma(\frac{1}{n})} \frac{v(t)}{2n\beta_0} \left(\frac{2\beta_0}{\beta(t)\Lambda(t)} \right)^{\frac{2}{n}}. \quad (10)$$

In these dimensionless units, the behavior of the underdamped Brownian particle depends only on the parameter α (the ratio of inertia memory and relaxation times), the potential parameter n , the normalized protocol $\Lambda(t)$ and the relative inverse temperature protocol $\beta(t)/\beta_0$.

Under ieq, the system will obey Boltzmann distribution of the Hamiltonian (1) with the distribution $\rho_{\text{ieq}}(x, p, t)$ factorized into the position distribution $P(x, t)$ and a Gaussian momentum distribution:

$$\rho_{\text{ieq}}(x, p, t) = P(x, t) P_G(p, \beta(t)),$$

$$P_G(p, \beta(t)) \equiv \sqrt{\frac{\alpha\beta(t)}{2\pi\beta_0}} e^{-\frac{\alpha\beta(t)}{2\beta_0} p^2}. \quad (11)$$

The mean work in the ieq process can then be computed theoretically (see Appendix A) to give

$$\langle W \rangle = \frac{1}{n} \int_0^\tau \frac{\dot{\Lambda}(t)}{\beta(t)\Lambda(t)} dt + W_{\text{diss}} \equiv \Delta\Phi + W_{\text{diss}}, \quad (12)$$

where $W_{\text{diss}} = \int_0^\tau dt \langle \frac{\partial U_1}{\partial t} \rangle$ is the mean dissipated work in the ieq process, and the quantity

$$\Delta\Phi \equiv \int_0^\tau dt \left\langle \frac{\partial U_0}{\partial t} \right\rangle = \int_0^\tau dt \dot{\lambda} \frac{\partial F}{\partial \lambda} = \int_0^\tau dt \left\langle \frac{\partial H_0}{\partial t} \right\rangle \quad (13)$$

can be interpreted as the mean work in the corresponding ramp process in the quasistatic limit (reversible). Thus the difference $\langle W \rangle - \Delta\Phi = W_{\text{diss}}$ is the dissipated (or irreversible) work of the ieq process. The mean heat of the ieq process can also be calculated using the First law of thermodynamics and the nature of ieq as

$$\langle Q \rangle = \Delta H_0 + \Delta U_1 - W_{\text{diss}} - \Delta\Phi \quad (14)$$

$$= \left(\frac{1}{2} + \frac{1}{n} \right) \Delta T + \Delta U_1 - W_{\text{diss}} - \Delta\Phi, \quad \text{where} \quad (15)$$

$$\Delta H_0 \equiv \langle H_0(\tau) \rangle - \langle H_0(0) \rangle,$$

$$\Delta U_1 \equiv \langle U_1(\tau) \rangle - \langle U_1(0) \rangle, \quad \Delta T \equiv T(\tau) - T(0). \quad (16)$$

Notice that the mean heat consists of the contribution from the kinetic energy change due to the temperature change [the $\Delta T/2$ term in (15)] and exists for both underdamped and overdamped dynamics [27].

III. TEMPERATURE AND STIFFNESS PROTOCOLS FOR MINIMAL DISSIPATION UNDER IEQ

Let us consider an ieq transition from $(\lambda(0), \beta(0)) \rightarrow (\lambda(\tau), \beta(\tau))$. Our goal is to find $\lambda(t)$ and $\beta(t)$ such that the dissipative work is minimal. Figure 1 shows a schematic picture of possible paths that connect the initial to the final states. There can be many different protocols that can connect the initial and final states (denoted by the black dashed curves), and each protocol can have its corresponding ieq transition. Among these different protocols, there is a protocol that has minimal dissipation under the ieq transition (denoted by the black solid curve). Here we consider the time-dependent protocols, $\lambda(t)$ and $\beta(t)$, which are functions of t/τ , i.e., a single timescale τ that characterizes the transition path. The mean dissipated work in the ieq process $W_{\text{diss}} = \int_0^\tau dt \langle \frac{\partial U_1}{\partial t} \rangle$ can be calculated to give (see Appendix A)

$$W_{\text{diss}} = \Delta U_1 + \int_0^\tau \mathcal{L}_n(\Lambda(t), \dot{\Lambda}(t), \beta(t), \dot{\beta}(t)) dt, \quad (17)$$

where

$$\mathcal{L}_n \equiv \frac{\alpha}{\beta} \left(\frac{v}{n} + \frac{\dot{\beta}}{2\beta} \right)^2 + \frac{1}{n^2\beta_0} \frac{\Gamma(\frac{3}{n})}{\Gamma(\frac{1}{n})} \left(\frac{2\beta_0}{\beta\Lambda} \right)^{\frac{2}{n}} v^2 \quad (18)$$

is the Lagrangian-like quantity and ΔU_1 can be calculated using (10). The mean heat can be obtained from (15) and (17) to give

$$\langle Q \rangle = \left(\frac{1}{2} + \frac{1}{n} \right) \Delta T - \frac{1}{n} \int_0^\tau \frac{\dot{\Lambda}(t)}{\beta(t)\Lambda(t)} dt - \int_0^\tau \mathcal{L}_n dt. \quad (19)$$

It is easy to see since \mathcal{L}_n is proportional to the square of the time-derivative of either β or Λ , a simple change of variable $t' = t/\tau$ in (18) leads to the scaling of $\int_0^\tau \mathcal{L}_n dt \propto 1/\tau$. It is also easy to see that ΔU_1 is $\propto 1/\tau$ and hence $W_{\text{diss}} \propto 1/\tau$. Since ΔU_1 is path independent, and thus $\int_0^\tau \mathcal{L}_n dt$ needs to be minimized if one aims to suppress dissipation, which is of particular relevance for fast processes. The optimal protocols for minimal W_{diss} are given by the Euler-Lagrange equations: $\frac{d}{dt} \left(\frac{\partial \mathcal{L}_n}{\partial \dot{\Lambda}} \right) = \frac{\partial \mathcal{L}_n}{\partial \Lambda}$ and $\frac{d}{dt} \left(\frac{\partial \mathcal{L}_n}{\partial \dot{\beta}} \right) = \frac{\partial \mathcal{L}_n}{\partial \beta}$. In the following, we will focus on the case of a harmonic potential with time-dependent stiffness. For the general nonharmonic potential of the form (4), similar approaches can be carried out. In this case, the mean of the auxiliary potential is

$$\langle U_1 \rangle = \frac{\dot{\beta}}{\beta^2} \left(\alpha + \frac{1}{4\Lambda} \right) + \frac{\dot{\Lambda}}{2\beta\Lambda} \left(\alpha + \frac{1}{2\Lambda} \right). \quad (20)$$

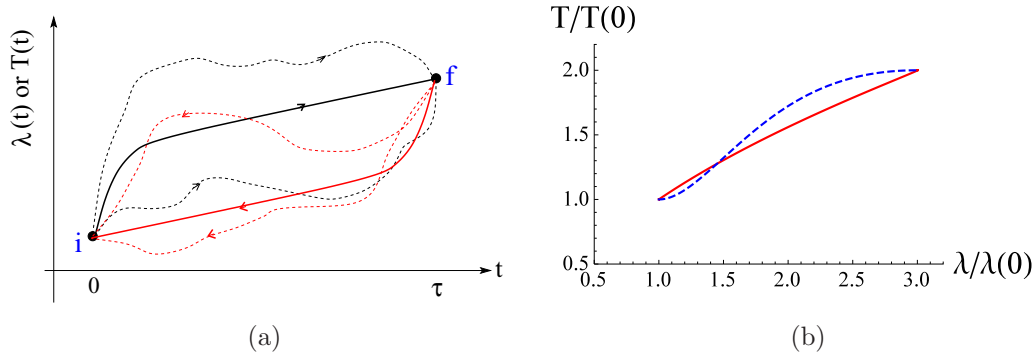


FIG. 1. (a) Schematic picture of transitions under time-dependent protocols. In general, there are many different protocols that can connect the initial and final states $i \rightarrow f$, denoted by the black dashed curves. And each protocol can have its corresponding ieq transition. Among these different protocols, there is a protocol that has minimal dissipation under the ieq transition, as denoted by the black solid curve. The backward transitions from $f \rightarrow i$ are also shown, the dashed red curve denotes an arbitrary protocol, and the solid red curve is the mdieq protocol. (b) mdieq transition paths on the λ - T plane for the cases in Fig. 2(a) (given temperature protocol $T(t)$ and $\lambda(t)$ is optimized, blue dashed curve) and Fig. 2(b) [both $T(t)$ and $\lambda(t)$ are optimized, red solid curve].

The Lagrangian for harmonic potential reduces to

$$\mathcal{L}_2 = \frac{1}{4\beta} \left[\alpha \left(v + \frac{\dot{\beta}}{\beta} \right)^2 + \frac{v^2}{\Lambda} \right], \tag{21}$$

and the corresponding Euler-Lagrange equations are

$$\left(\alpha + \frac{1}{\Lambda(t)} \right) \dot{v}(t) - \frac{v^2(t)}{2\Lambda(t)} + \alpha \frac{\ddot{\beta}(t)}{\beta(t)} - \alpha \frac{\dot{\beta}(t)}{\beta(t)} \left(v(t) + \frac{2\dot{\beta}(t)}{\beta(t)} \right) = 0, \tag{22}$$

$$\left(2\alpha + \frac{1}{\Lambda(t)} \right) \dot{v}(t) + \frac{1}{2} \left(\alpha - \frac{1}{\Lambda(t)} \right) v^2(t) + 2\alpha \frac{\ddot{\beta}(t)}{\beta(t)} - \alpha \frac{\dot{\beta}(t)}{\beta(t)} \left(v(t) + \frac{7\dot{\beta}(t)}{2\beta(t)} \right) = 0, \tag{23}$$

where $v(t) \equiv \frac{\dot{\beta}(t)}{\beta(t)} + \frac{\dot{\Lambda}(t)}{\Lambda(t)}$. (22) and (23) are solved with the fixed end-points B.C.s

$$\beta(t=0) = \beta(0), \beta(t=\tau) = \beta(\tau); \quad \Lambda(t=0) = \Lambda(0), \Lambda(t=\tau) = \Lambda(\tau) \tag{24}$$

to give the minimal dissipation ieq (mdieq) protocols $\lambda^*(t)$ and $\beta^*(t)$. One can show that if $\dot{\beta} \neq 0$ (see Appendix B) then

$$-\frac{1}{2} \int_0^\tau \mathcal{L}_2(\lambda^*(t), \dot{\lambda}^*(t), \beta^*(t), \dot{\beta}^*(t)) dt = \Delta U_1^* \equiv \langle U_1^*(\tau) \rangle - \langle U_1^*(0) \rangle, \tag{25}$$

where U_1^* denotes the auxiliary potential with the mdieq protocols, and the asterisk is used to denote quantities or protocols under the mdieq condition. Hence the minimal dissipation and the associated mean work and heat [using (15)] are simply given by

$$W_{\text{diss}}^* = \Delta U_1^* + \int_0^\tau \mathcal{L}_2^* dt = -\Delta U_1^* = \frac{1}{2} \int_0^\tau \mathcal{L}_2^* dt, \tag{26}$$

$$\langle W^* \rangle = \Delta \Phi^* - \Delta U_1^*, \quad \Delta \Phi^* = \frac{1}{2} \int_0^\tau \frac{\dot{\lambda}}{\lambda \beta} dt, \tag{27}$$

$$\langle Q^* \rangle = \Delta T - \Delta \Phi^* + 2\Delta U_1^* \quad \text{for } \dot{\beta} \neq 0. \tag{28}$$

On the other hand, if $\dot{\beta} = 0$ (temperature is fixed), $W_{\text{diss}}^* \neq -\Delta U_1^*$, but W_{diss}^* and $\langle Q^* \rangle$ can be explicitly calculated [see Eqs. (33) and (34) below]. It is worth noting that $\Delta U_1^* < 0$ if the initial and final states are distinct, i.e., the minimal dissipation requirement renders a decrease in the auxiliary potential so as to suppress the dissipation.

The mdieq protocols for arbitrary initial and final states can be obtained by solving the boundary-value ODEs (22) and

(23) numerically, say using the shooting method. Figure 2(a) shows the case of the given temperature protocol $T(t) = T(0) + \frac{\Delta T}{2}(1 - \cos \frac{\pi t}{\tau})$ with $T(\tau)/T(0) = 2$. The optimal $\lambda(t)$ is obtained by numerically solving (22) with the B.C. $\lambda(\tau)/\lambda(0) = 3$, with the minimized dissipation $\beta(0)W_{\text{diss}}^* = 0.0206035$. On the other hand, if now both $\lambda(t)$ and $\beta(t)$ can be varied to minimize W_{diss} , then (22) and (23) are solved simultaneously to give the mdieq protocols $\lambda^*(t)$ and $\beta^*(t)$ and the results are shown in Fig. 2(b). In this case, $\beta(0)W_{\text{diss}}^* = 0.0156259$, which is significantly less than the previous case. The corresponding mdieq paths in the λ - T plane are shown in Fig. 1(b). The minimized dissipation work is shown as a function of $\lambda(\tau)/\lambda(0)$ for $\alpha = 1$ and 0.1 in Figs. 2(c) and 2(e) for the cases of $T(\tau)/T(0) = 2$ and $1/2$, respectively. In general the minimized W_{diss}^* is always positive and increases with the inertia factor α . The corresponding $\Delta \Phi^*$ are also shown. The mean work and heat under mdieq for the cases of Figs. 2(c) and 2(e) are shown respectively in Figs. 2(d) and 2(f). It is clear that in the case of cooling [Fig. 2(f)], the mean work can be negative in some regimes indicating that work

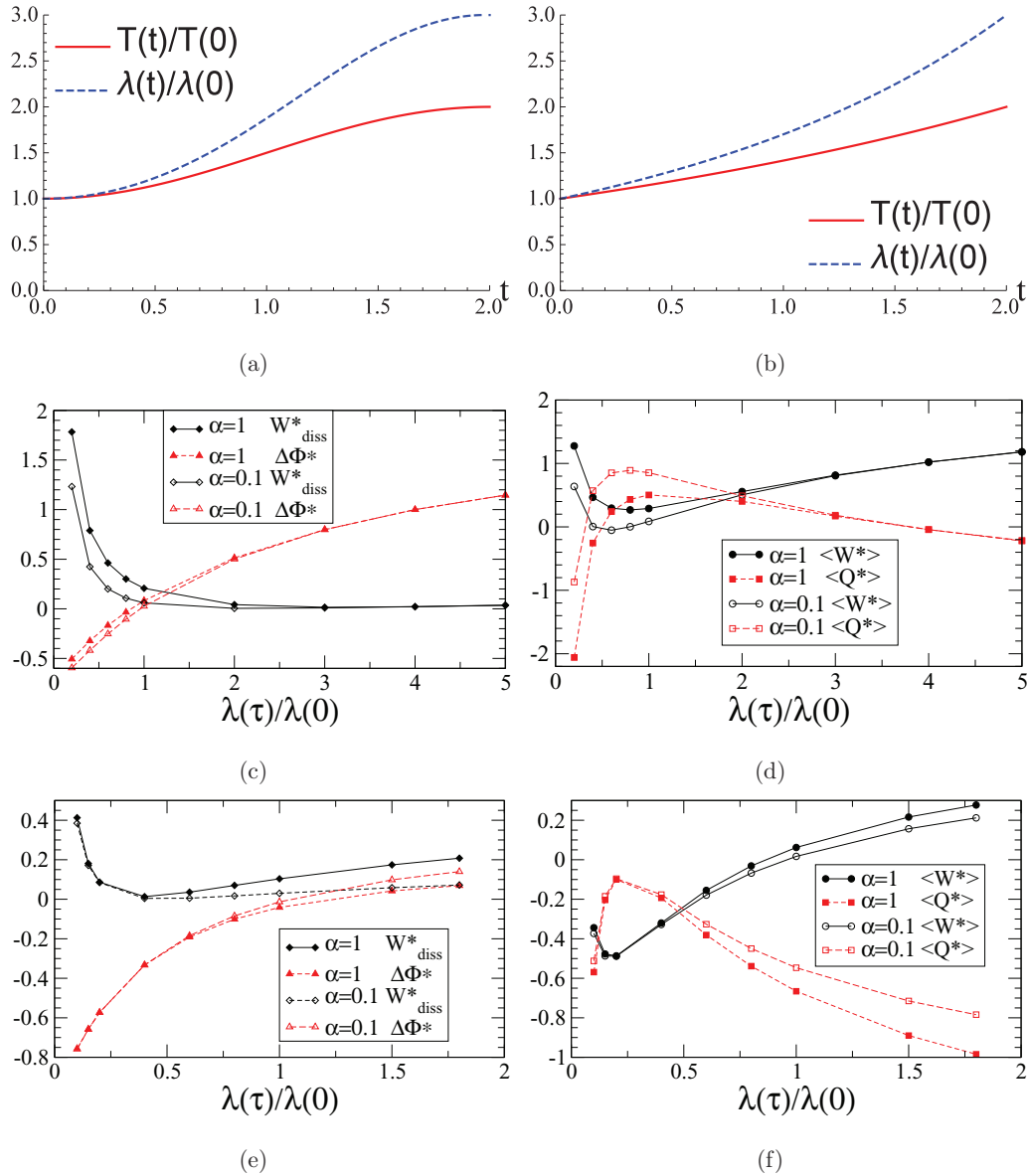


FIG. 2. mdieq transition of an underdamped Brownian particle under the time-dependent harmonic potential $U_0(x, \lambda(t)) = \frac{1}{2}\lambda(t)x^2$. (a) Optimal $\lambda(t)$ for given temperature protocol $T(t) = T(0) + \frac{\Delta T}{2}(1 - \cos \frac{\pi t}{2})$ with $T(\tau)/T(0) = 2$. $\lambda(t)$ is optimized with $\lambda(\tau)/\lambda(0) = 3$. $\beta(0)W_{\text{diss}}^* = 0.0206035$. (b) Both $T(t)$ and $\lambda(t)$ are optimized with $T(\tau)/T(0) = 2$ and $\lambda(\tau)/\lambda(0) = 3$. $\beta(0)W_{\text{diss}}^* = 0.0156259$. (c) Minimal dissipative work and $\Delta\Phi^*$ as a function of $\lambda(\tau)/\lambda(0)$ for $T(\tau)/T(0) = 2$ (heating up). (d) The mean work and heat as a function of $\lambda(\tau)/\lambda(0)$ for the case in (c). (e) W_{diss}^* and $\Delta\Phi^*$ as a function of $\lambda(\tau)/\lambda(0)$ for $T(\tau)/T(0) = 1/2$ (cooling). (f) The mean work and heat for the case in (e).

can be extracted under mdieq, with the corresponding heat being flowed out of the system. Several analytic results for the mdieq transition can be derived, as shown in the following sections.

A. Minimal dissipation ieq paths with reversed initial and final states

For given initial and final states (denoted by i and f), in general there are many different sets of protocols $(\lambda(t), \beta(t))$ that can connect $i \rightarrow f$ (see Fig. 1). And each set of protocols can have its corresponding ieq transition specified

by the action of $U_0(x, \lambda(t)) + U_1(x, p, \lambda(t), \beta(t), \dot{\lambda}(t), \dot{\beta}(t))$. Similarly, there are also many different sets of protocols $(\lambda_r(t), \beta_r(t))$ that can connect backward from $f \rightarrow i$ (or reverse process, denoted by the subscript r), and each one can have its own ieq transition (ieqr), as shown schematically in Fig. 1. In general, the backward protocol $(\lambda_r(t), \beta_r(t))$ is not related to the forward ones. Remarkably, the *optimized* mdieq transition restores the time-reversal symmetry of the protocols, i.e., the ieq minimal dissipative condition selects the forward protocol and backward protocol to be time-reversal related. In addition, the ieq forward and ieq backward minimal dissipative works are the same (see Appendix C for

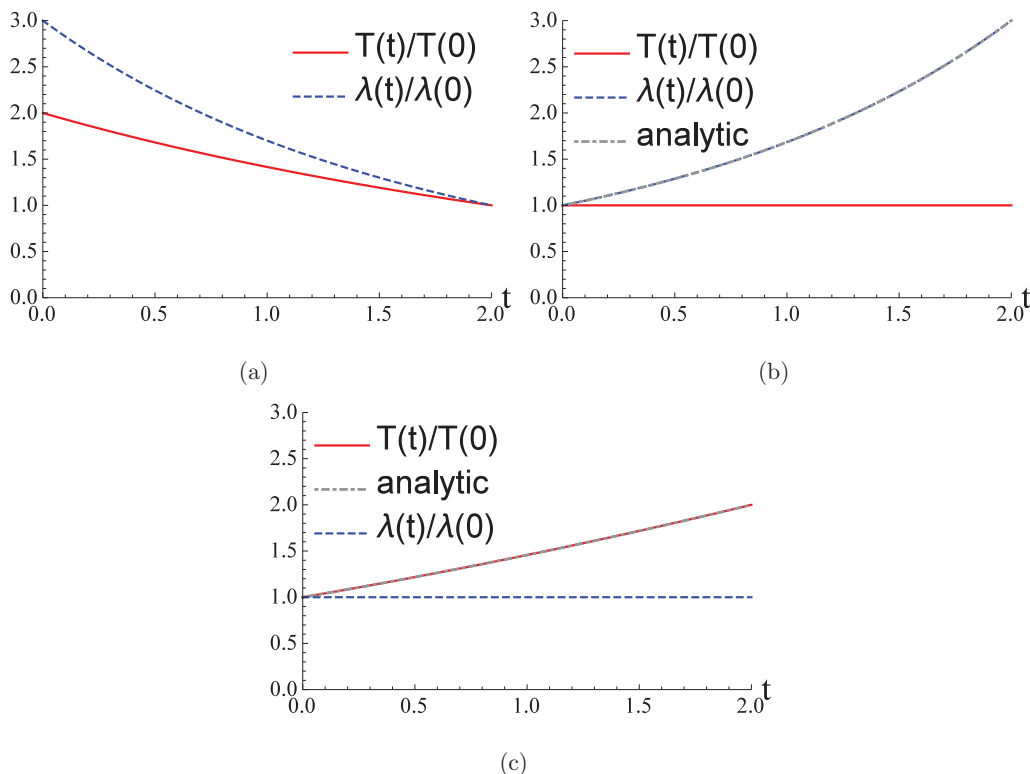


FIG. 3. Optimal protocols for the transition of an underdamped Brownian particle ($\alpha = 1$) under ieq under the time-dependent harmonic potential $U_0(x, \lambda(t)) = \frac{1}{2}\lambda(t)x^2$. The mdieq protocols are obtained from the numerical solutions of (22) and (23). (a) The optimized protocols for the case of exchanging the initial and final states in Fig. 2(b). Notice that the optimized protocols are exactly the time reversal protocols in Fig. 2(b). (b) T fixed and $\lambda(\tau)/\lambda(0) = 3$. $\beta(0)W_{\text{diss}} = 0.224099$. The analytic result (32) is also shown (dot-dashed curve). (c) λ fixed and $T(\tau)/T(0) = 2$. $\beta(0)W_{\text{diss}} = 0.214466$. The analytic result (36) is also shown (dot-dashed curve).

derivations):

$$\lambda_r^*(t) = \lambda^*(\tau - t), \quad \beta_r^*(t) = \beta^*(\tau - t); \quad (29)$$

$$W_{\text{diss}r}^* = W_{\text{diss}}^*. \quad (30)$$

Figure 3(a) shows the mdieq protocols with $T(\tau)/T(0) = 1/2$ and $\lambda(\tau)/\lambda(0) = 1/3$ which is exactly the case in Fig. 2(b) but with the initial and final states exchanged, i.e., its backward mdieq process. It is clear that the mdieq protocols are exactly the time-reversal of the mdieq protocols of the forward process in Fig. 2(b). In addition, the minimized $\beta(0)W_{\text{diss}r}^* = 0.0156259$, which is the same as the forward W_{diss}^* , verifying (30).

It should be noted that as in general ieq transition [27], because of the odd-parity of the time derivatives in U_1 , the mdieq transition phase space trajectory of the backward process is not the time reversal of the mdieq transition of the forward process. However, because of the ieq nature, namely, the distribution being Boltzmann with parameters depending on the instantaneous values of $(\lambda^*(t), \beta^*(t))$, the distribution function of the backward mdieq paths is the same as the time reversal of the forward mdieq distribution: $\rho_{\text{mdieq}r}(x, p, t) = \rho_{\text{mdieq}f}(x, p, \tau - t)$, i.e., time-reversal symmetry is restored under the ensemble of the trajectories.

B. Pure temperature change and pure potential change mdieq protocols

We shall consider two simpler special classes of mdieq processes. The first is the case of no variation in temperature, $\beta = 0$, i.e., the only time variation of the potential stiffness. The Euler-Lagrange equation (22) then reduces to

$$\ddot{\Lambda} = \dot{\Lambda}^2 \frac{2\alpha\Lambda + 3}{2\Lambda(\alpha\Lambda + 1)}, \quad (31)$$

which can be solved analytically with the B.C.s (24) for the mdieq protocol Λ^* whose time-dependence is given by the following implicit expression

$$\begin{aligned} \sqrt{\alpha\Lambda^*} &= \sinh\left(\sqrt{1 + \frac{1}{\alpha\Lambda^*}} + c_1 - c_2 \frac{t}{\tau}\right), \quad \text{where} \\ c_1 &= \sinh^{-1}\sqrt{\alpha\Lambda(0)} - \sqrt{1 + \frac{1}{\alpha\Lambda(0)}}, \\ c_2 &= c_1 + \sqrt{1 + \frac{1}{\alpha\Lambda(\tau)}} - \sinh^{-1}\sqrt{\alpha\Lambda(\tau)}. \end{aligned} \quad (32)$$

The minimal dissipation can be explicitly calculated to give

$$W_{\text{diss}}^* = \Delta U_1^* + \frac{\alpha c_2^2}{\beta\tau} = \frac{\alpha c_2}{\beta\tau} \left(\frac{1 + \frac{1}{2\alpha\Lambda(0)}}{\sqrt{1 + \frac{1}{\alpha\Lambda(0)}}} - \frac{1 + \frac{1}{2\alpha\Lambda(\tau)}}{\sqrt{1 + \frac{1}{\alpha\Lambda(\tau)}}} + c_2 \right). \quad (33)$$

Note that ΔU_1^* is always negative if $\Lambda(0) \neq \Lambda(\lambda)$. Also, Λ^* is independent of the value of the fixed temperature, and βW_{diss}^* depends only on α (increases with α) and the end points of Λ . The mean heat under mdieq can be calculated from (19) to give

$$\langle Q^* \rangle = - \left(\frac{1}{2} \ln \frac{\lambda(\tau)}{\lambda(0)} + \frac{\alpha c_2^2}{\tau} \right) T. \quad (34)$$

Figure 3(b) shows the mdieq protocol of $\lambda^*(t)$ for the case of fixed temperature obtained from the numerical solution of (22). The analytic result from (32) is also plotted, showing perfect agreement.

The second case is that there is no variation in λ , $\dot{\Lambda} = 0$, i.e., the potential remained fixed and only the temperature changed. The Euler-Lagrange equation (23) can be simplified to

$$\ddot{\beta} = \frac{3}{2} \frac{\dot{\beta}^2}{\beta}, \quad (35)$$

which can be solved to give the mdieq temperature protocol

$$\frac{T^*(t)}{T(0)} = \left[1 + \left(\sqrt{\frac{T(\tau)}{T(0)}} - 1 \right) \frac{t}{\tau} \right]^2. \quad (36)$$

The minimal dissipation, mean work and heat can be derived to give

$$\langle W^* \rangle = W_{\text{diss}}^* = \frac{4\alpha + \frac{1}{\Lambda}}{2\tau} \left(\sqrt{\frac{T(\tau)}{T(0)}} - 1 \right)^2 T(0), \quad (37)$$

$$\langle Q^* \rangle = \Delta T - \frac{4\alpha + \frac{1}{\Lambda}}{\tau} \left(\sqrt{\frac{T(\tau)}{T(0)}} - 1 \right)^2 T(0). \quad (38)$$

Note that $T^*(t)$ is independent of α and the value of λ . Figure 3(c) shows the mdieq protocol of $T^*(t)$ for the case of fixed λ obtained from the numerical solution of (23). The analytic formula (36) is also plotted, showing perfect agreement.

C. the minimal dissipation ieq protocol is isentropic

It has been shown [27] that it is possible to design ieq transition that is isentropic, i.e., the entropy stays constant along the ieq path, by imposing the isentropic condition $\lambda(t)\beta^2(t) = \lambda(0)\beta^2(0)$. In addition, it is also possible to achieve a zero entropy change ieq transition such that there is no entropy change between the initial and final states, but the instantaneous entropy can vary during the ieq transition. The zero entropy change condition is less restrictive, and it only requires $\lambda(\tau)\beta^2(\tau) = \lambda(0)\beta^2(0)$.

With the isentropic condition, the Euler-Lagrange equations (22) or (23) can be simplified to

$$\ddot{\beta} = \frac{\beta^2}{2\beta}, \quad (39)$$

whose solution can be derived to be

$$\frac{T_{\text{isen}}^*(t)}{T(0)} = \left[1 - \left(1 - \sqrt{\frac{T(0)}{T(\tau)}} \right) \frac{t}{\tau} \right]^{-2}. \quad (40)$$

The minimal dissipation and heat are given by

$$W_{\text{diss}}^{*(\text{isen})} = \frac{1}{2\tau} \left(\sqrt{\frac{T(0)}{T(\tau)}} - 1 \right)^2 T(0), \quad (41)$$

$$\langle Q_{\text{isen}}^* \rangle = - \frac{1}{\tau} \left(\sqrt{\frac{T(0)}{T(\tau)}} - 1 \right)^2 T(0). \quad (42)$$

Notice that the optimal isentropic protocol, the corresponding $W_{\text{diss}}^{*(\text{isen})}$ and $\langle Q_{\text{isen}}^* \rangle$ are all independent of α . One can take the solution of $T_{\text{isen}}^*(t)$ in (40) and $\lambda_{\text{isen}}^*(t) = \lambda(0)(T_{\text{isen}}^*(t)/T(0))^2$, and substitute directly into (22) and (23) to verify that this is indeed the optimal solution. Remarkably, if the initial and final states are consistent with the zero entropy change condition [27], namely, $\lambda(\tau)\beta^2(\tau) = \lambda(0)\beta^2(0)$, then the mdieq path is automatically isentropic. One can also obtain the numerical solutions for the mdieq protocol with the initial and final states compatible with the zero entropy change condition, as shown in Fig. 4 together with the analytic isentropic ieq path (40), verifying indeed the mdieq path is also the ieq isentropic protocol. Thus, in some sense, the minimal dissipation condition forces the ieq path to become isentropic, which is in agreement with the intuition (as in the quasistatic case) that the constant entropy path has the lowest dissipation. Fig. 4(c) shows the isentropic ieq path in the λ - T plane. Two other zero entropy change mdieq paths, one with a constant λ portion and another with a constant T portion [having $\beta(0)W_{\text{diss}}^* = 0.51303$ and 0.41156 , respectively], are also shown. The two zero entropy change mdieq paths have minimal dissipative work that are considerably larger than that of the isentropic mdieq path [with $\beta(0)W_{\text{diss}}^{*(\text{isen})} = 0.0144198$].

D. Work extraction in mdieq transitions

As revealed in Fig. 2(f), it is possible to extract work under mdieq transitions. For work extraction, $\langle W^* \rangle = \Delta\Phi^* + W_{\text{diss}}^* < 0$. Since W_{diss}^* is always non-negative, one requires $\Delta\Phi^* < 0$. For the case of pure temperature change and no change in stiffness $\lambda = 0$, $\Delta\Phi \equiv 0$, hence $\langle W^* \rangle = W_{\text{diss}}^* \geq 0$ and it is impossible to extract work. The power delivered during the mdieq transition is $P^* = -\langle W^* \rangle/\tau$, which has a τ dependence of the form $P^* = A/\tau - B/\tau^2$, where the positive constants A and B can be readily calculated. It is then easy to show that work can be extracted from the mdieq engine with a positive power $P^* > 0$ for $\tau > \tau_c = B/A$. Furthermore, the transition path has a maximal power $P_{\text{max}}^* = A^2/(4B) > 0$ at $\tau_{\text{max}} = 2B/A = 2\tau_c$. In the following, we focus on the mdieq transition discussed in the previous sections.

For the case of pure stiffness variation and no temperature change $\dot{T} = 0$, since $\Delta\Phi = \frac{T}{2} \ln \frac{\lambda(\tau)}{\lambda(0)}$ and $W_{\text{diss}}^* > 0$, hence

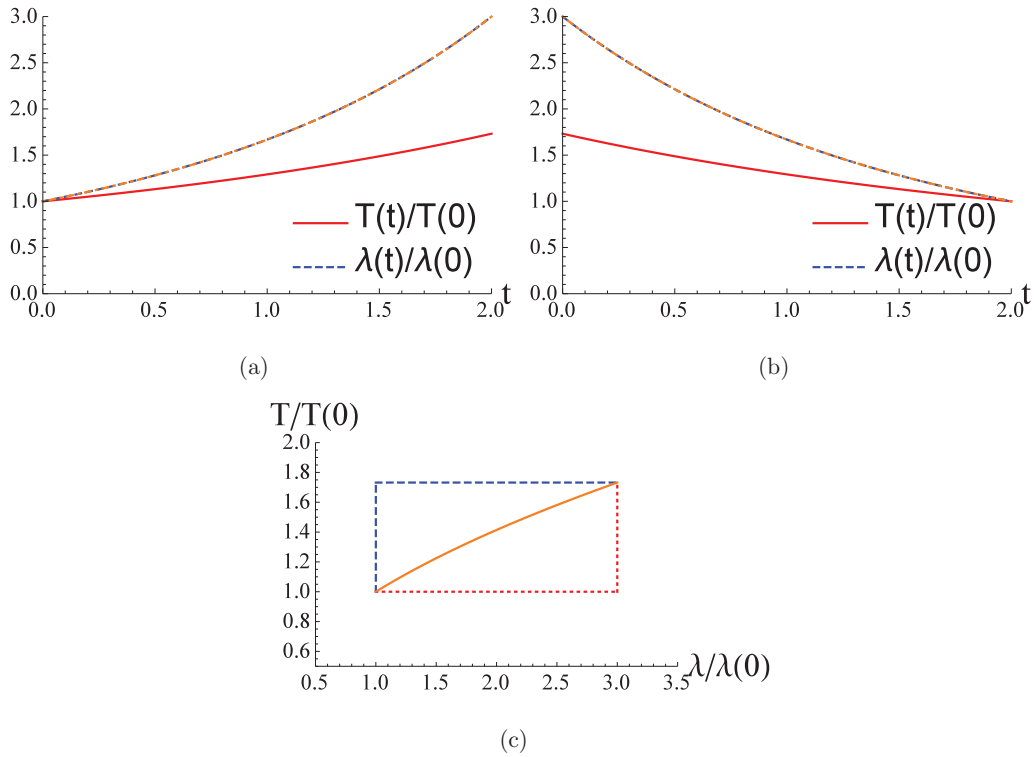


FIG. 4. Optimal protocols for the transition of an underdamped Brownian particle ($\alpha = 1$) under icq under the time-dependent harmonic potential $U_0(x, \lambda(t)) = \frac{1}{2}\lambda(t)x^2$. (a) $T(t)$ and $\lambda(t)$ are optimized with $T(\tau)/T(0) = \sqrt{3}$ and $\lambda(\tau)/\lambda(0) = 3$ [obtained from the numerical solutions of (22) and (23)], which is compatible with the isentropic condition. The isentropic curve of $\lambda(t) = \lambda(0)(\frac{T^*(t)}{T(0)})^2$ is also shown (orange dot-dashed curve), which coincides with the optimized $\lambda^*(t)$. $\beta(0)W_{\text{diss}}^{*(\text{isen})} = 0.0144198$. (b) Similar to (a) but for the reverse (cooling) process with $T(\tau)/T(0) = 1/\sqrt{3}$ and $\lambda(\tau)/\lambda(0) = 1/3$. $\beta(0)W_{\text{diss}}^{*(\text{isen})} = 0.0144198$ also, verifying (30). (c) mdieq isentropic path on the λ - T plane for the case in (a) (orange solid curve). Two other mdieq paths (blue dashed curve at a higher temperature and red dotted curve at a lower temperature) each consisting of a constant T and a constant λ portion are also shown for comparison. $\beta(0)W_{\text{diss}}^* = 0.51303$ and 0.41156 respectively for the blue dashed and red dotted paths respectively.

work can be extracted only for the case of compression, i.e., $\lambda(\tau) < \lambda(0)$. Using (33), the mean work in this case is

$$\langle W^* \rangle = \frac{T}{2} \ln \frac{\lambda(\tau)}{\lambda(0)} + \frac{\alpha c_2 T}{\tau} \left(c_2 + \frac{1 + \frac{1}{2\alpha}}{\sqrt{1 + \frac{1}{\alpha}}} - \frac{1 + \frac{\lambda(0)}{2\alpha\lambda(\tau)}}{\sqrt{1 + \frac{\lambda(0)}{\alpha\lambda(\tau)}}} \right), \tag{43}$$

and it is easy to see that $\langle W^* \rangle$ is positive for $\frac{\lambda(\tau)}{\lambda(0)} > 1$. The dependence of $\langle W^* \rangle$ as a function of $\frac{\lambda(\tau)}{\lambda(0)}$ is shown in Fig. 5(a) for various values of α and τ . $\langle W^* \rangle$ is negative in some compression regime and there is a minimal negative $\langle W^* \rangle_{\text{min}}$ indicating there is an optimal choice of $(\frac{\lambda(\tau)}{\lambda(0)})_{\text{min}}$ for maximal work extraction. The optimal ratio $\frac{\lambda(\tau)}{\lambda(0)}$ increases with α along with a decrease with the maximal extracted work, as shown in Fig. 5(a). The mean power given by $P^* = -\langle W^* \rangle/\tau$ is plotted as a function of τ in Fig. 5(b), displaying a maximum power P_{max}^* at some τ_{max} . One can easily show that

$$P^* = T \left(\frac{A}{\tau} - \frac{B}{\tau^2} \right), \quad \text{where} \tag{44}$$

$$A \equiv \frac{1}{2} \ln \frac{\lambda(0)}{\lambda(\tau)}, \quad B \equiv \alpha c_2 \left(c_2 + \frac{1 + \frac{1}{2\alpha}}{\sqrt{1 + \frac{1}{\alpha}}} - \frac{1 + \frac{\lambda(0)}{2\alpha\lambda(\tau)}}{\sqrt{1 + \frac{\lambda(0)}{\alpha\lambda(\tau)}}} \right), \tag{45}$$

$$\tau_{\text{max}} = \frac{2B}{A}, \quad P_{\text{max}}^* = \frac{A^2}{4B}. \tag{46}$$

Finally, for the case of isentropic mdieq, since $\beta^{*2}\lambda^* = \text{constant}$, hence $\Delta\Phi^* = \Delta T$ and using (41), the mean work is

$$\langle W^* \rangle = T(\tau) - T(0) + \frac{T(0)}{2\tau} \left(\sqrt{\frac{T(0)}{T(\tau)}} - 1 \right)^2, \tag{47}$$

which is independent of α . It is easy to see that $\langle W^* \rangle < 0$ and work extraction is possible only for in some appropriate cooling (and also expansion due to the isentropic condition) range given by $\frac{\sqrt{1+8\tau}-1}{4\tau} < \frac{T(\tau)}{T(0)} < 1$. Figure 6(a) shows $\langle W^* \rangle$ as a function of $\frac{T(\tau)}{T(0)}$ for various values of τ . Furthermore, one can show that $\langle W^* \rangle$ always has a negative minimum

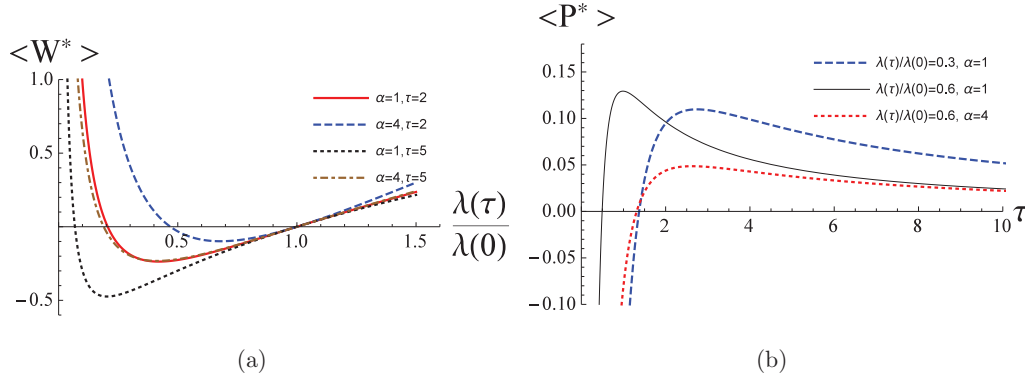


FIG. 5. (a) mdieq mean work, $\langle W^* \rangle$ (in unit of the fixed temperature), as a function of $\frac{\lambda(\tau)}{\lambda(0)}$ for the case of stiffness change and fixed temperature. (b) The mdieq mean power extracted as a function of τ . for the case in (a).

of $\langle W^* \rangle_{\min}$ at

$$\left(\frac{T(\tau)}{T(0)}\right)_{\min} = \left[\frac{1 + \sqrt{1 + \frac{4}{27\tau}}}{2\tau}\right]^{\frac{1}{3}} - \frac{1}{3} \left[\frac{2}{\tau^2} \frac{1}{1 + \sqrt{1 + \frac{4}{27\tau}}}\right]^{\frac{1}{3}}. \quad (48)$$

Figure 6(b) plots $\left(\frac{T(\tau)}{T(0)}\right)_{\min}$ and the minimal mean work $\langle W^* \rangle_{\min}$ as a function of τ . The mean power P^* as a function of τ is plotted in Fig. 6(c) also displaying a maximum power P_{\max}^* at some τ_{\max} whose explicit expression can be derived to be

$$\tau_{\max} = \frac{T(0)}{T(\tau)} \left(\frac{\sqrt{T(0)} - \sqrt{T(\tau)}}{\sqrt{T(0)} + \sqrt{T(\tau)}} \right), \quad P_{\max}^* = \frac{T(\tau)}{2} \left(1 + \sqrt{\frac{T(\tau)}{T(0)}} \right)^2. \quad (49)$$

E. Overdamped limit of the mdieq transition

Since the minimal dissipative work decreases with decreasing α [see Figs. 2(e) and 2(f), (33) and (37)] and will be lowest in the overdamped $\alpha \rightarrow 0$ limit. Furthermore, many experimental systems, such as the Brownian colloids, are operated in the overdamped regime, thus here we consider the mdieq transition in the overdamped limit which presumably has a good chance to be realized experimentally.

Taking the overdamped $\alpha \rightarrow 0$ limit in (6), $\beta_0 U_1 = \frac{1}{4} \left(\frac{\dot{\lambda}(t)}{\lambda(t)} + \frac{\dot{\beta}(t)}{\beta(t)} \right) x^2 \equiv \frac{v(t)}{4} x^2$, and the total potential for the mdieq paths can be written explicitly as

$$\beta_0 U_{\text{ieq}}(x, t) = \frac{1}{2} \left(\Lambda(t) + \frac{1}{2} v(t) \right) x^2. \quad (50)$$

Under the overdamped limit, the two Euler Lagrange equations (22) and (23) reduce to a single equation

$$\dot{v} = \frac{v^2}{2}, \quad (51)$$

which can be integrated to give the relation between the mdieq protocol pairs

$$\beta^*(t) \Lambda^*(t) = \frac{\beta(0) \Lambda(0)}{\left[1 + \chi \frac{t}{\tau}\right]^2}, \quad \chi \equiv \sqrt{\frac{\beta(0) \lambda(0)}{\beta(\tau) \lambda(\tau)}} - 1. \quad (52)$$

It is worth to note that in the $\alpha \rightarrow 0$ limit, the two Euler-Lagrange equations degenerate into a single equation resulting

in the freedom to choose $\beta(t)$ and $\lambda(t)$ from a family of (infinitely many) protocol pairs compatible with the given initial and final states that satisfy (52). The above still holds for general nonharmonic potentials given by (4) [38]. Hence we have the flexibility to choose a variety of desirable or convenient mdieq protocols. For instance, one can choose the constant stiffness (isochoric) protocol [$\lambda^*(t) = \lambda(0) = \lambda(\tau)$], then (52) reduces to (36) as expected. If one chooses the isothermal protocol, then by taking the $\alpha \rightarrow 0$ limit [39] in (32), one obtains the same result (52) with $\beta^*(t) = \beta(0) = \beta(\tau)$. Likewise, if one chooses the isentropic protocol [$\beta^* \Lambda^* = \beta^2(0) \Lambda(0) = \beta^2(\tau) \Lambda(\tau)$], then (52) reduces to (40) as in previous section.

The energetics can be explicitly computed in the overdamped limit. The total potential under mdieq condition is then given by

$$\beta_0 U_{\text{ieq}}^*(x, t) = \frac{1}{2} \left(\Lambda^*(t) - \frac{\chi}{\tau \left[1 + \chi \frac{t}{\tau}\right]} \right) x^2. \quad (53)$$

The mean auxiliary potential is

$$\langle U_1 \rangle = \frac{v}{4\beta\Lambda} = \frac{1}{4\beta\Lambda} \frac{d \ln[\beta\Lambda]}{dt}, \quad (54)$$

and using (52), we have

$$\langle U_1^* \rangle = -\frac{T(0)}{2\tau\Lambda(0)} \chi \left(1 + \chi \frac{t}{\tau} \right) \quad (55)$$

$$\Rightarrow \Delta U_1^* = -\frac{T(0)}{2\tau\Lambda(0)} \chi^2. \quad (56)$$

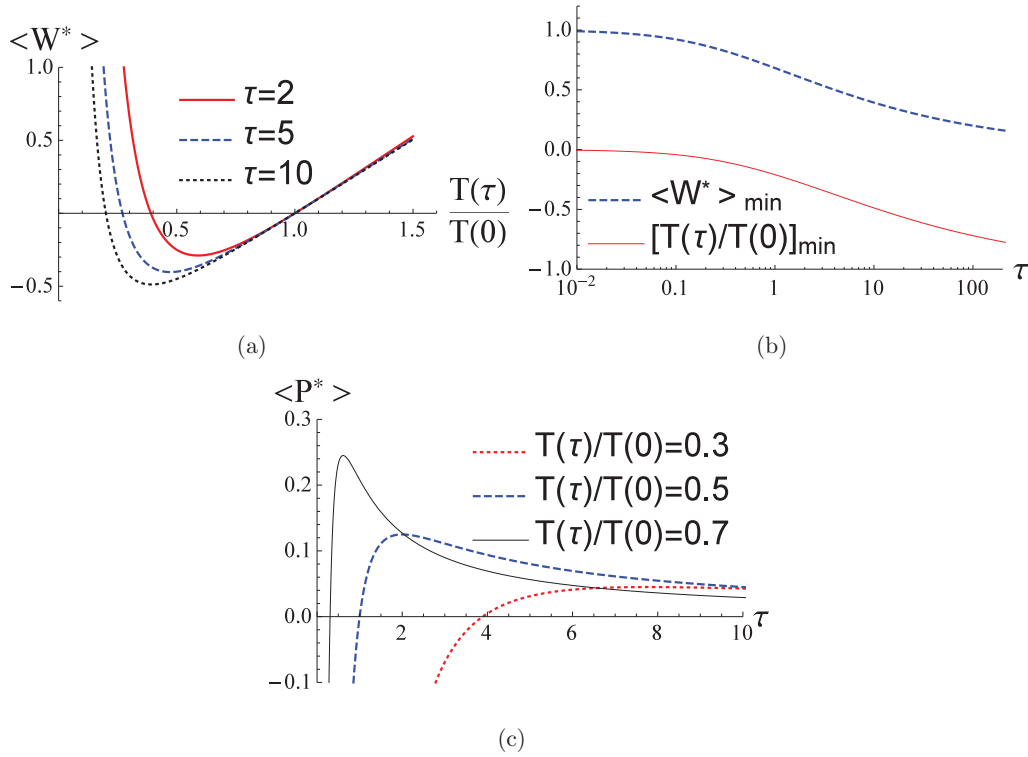


FIG. 6. (a) Isentropic mdieq mean work, $\langle W^* \rangle$ [in unit of $T(0)$], as a function of $\frac{T(\tau)}{T(0)}$. (b) $(\frac{T(\tau)}{T(0)})_{\min}$ and the minimal mean work $\langle W^* \rangle_{\min}$ as a function of τ . (c) The mdieq mean power extracted as a function of τ for the case in (a).

Using the relation $\mathcal{L}_2 = \frac{v^2}{4\beta\Lambda}$ in the overdamped limit and (52), one can get $\int_0^\tau \mathcal{L}_2^* dt = -2\Delta U_1^*$ and hence

$$W_{\text{diss}}^* = -\Delta U_1^* = T(0) \frac{\chi^2}{2\tau\Lambda(0)} \geq 0, \quad (57)$$

exemplifying a positive dissipative work if the initial and final states are distinct. Finally, $\Delta\Phi^*$ can be directly calculated to give

$$\begin{aligned} \Delta\Phi^* &= \frac{1}{2} \int_0^\tau \frac{\dot{\Lambda}^*}{\beta^* \Lambda^*} dt & (58) \\ &= \frac{T(0)}{2\lambda(0)} \int_0^\tau \dot{\lambda}^*(t) \left(1 + \chi \frac{t}{\tau}\right)^2 dt. & (59) \end{aligned}$$

To illustrate the flexibility and great freedom to choose the mdieq protocols, we consider the following protocols for $\lambda^*(t)$: (i) $\lambda^*(t) = \lambda(0) + \frac{\Delta\lambda}{2}(1 - \cos \frac{\pi t}{\tau})$, (ii) $\lambda^*(t) = \lambda(0) + \Delta\lambda(3 - 2\frac{t}{\tau})(\frac{t}{\tau})^2$, (iii) $\lambda^*(t) = \lambda(0) + 6\Delta\lambda(\frac{t}{\tau})^2 - \frac{5}{2}\frac{t}{\tau} + \frac{5}{3})(\frac{t}{\tau})^3$, and (iv) $\lambda^*(t) = \lambda(0) + \Delta\lambda(\frac{t}{\tau})^\mu$, ($\mu > 0$). The above $\lambda^*(t)$ protocols are shown in Fig. 7(a) and the paths in the λ - T plane are displayed in Fig. 7(b). The mdieq protocols for the underdamped cases, which do not have the freedom to choose, are also shown for comparison.

The mean work and heat are given by $\langle W^* \rangle = \Delta\Phi^* - \Delta U_1^*$ and $\langle Q^* \rangle = \Delta T - \Delta\Phi^* + 2\Delta U_1^*$ respectively, which can be derived as a function of $\frac{T(\tau)}{T(0)}$ and $\frac{\lambda(\tau)}{\lambda(0)}$ for given $\lambda^*(t)$ using (56) and (59). Assuming a single timescale in the protocol $\lambda^*(t)$ can be put into the form $\lambda^*(t) = \tilde{\lambda}^*(\frac{t}{\tau})$, then $\langle W^* \rangle$

can be expressed as

$$\frac{\langle W^* \rangle}{T(0)} = \frac{1}{2\lambda(0)} \int_0^1 \dot{\tilde{\lambda}}^*(y) [1 + \chi y]^2 dy + \frac{\chi^2}{2\tau}. \quad (60)$$

Here we are also interested in the scenario that work can be extracted from the mdieq path. Similar analysis as in the underdamped case reveals that $\langle W^* \rangle < 0$ is possible only for the case of expansion, and more work can be extracted if $\lambda^*(t)$ is monotonically decreasing. Figure 8(a) plots $\langle W^* \rangle$ as a function of $\frac{T(\tau)}{T(0)}$ for the mdieq transition in the overdamped limit for the protocols (i)–(iv) with the same expansion ratio of $\frac{\lambda(0)}{\lambda(\tau)} = 3$. In general, there is a significant regime in which work can be extracted ($\langle W^* \rangle < 0$). Also there exists a local minimum for $\langle W^* \rangle$ as a function of $\frac{T(\tau)}{T(0)}$ for a given of $\frac{\lambda(\tau)}{\lambda(0)}$. The above observation can be further established theoretically by examining the expression in (60). (60) reveals that $\langle W^* \rangle$ is a quadratic function of the parameter $\chi \equiv \sqrt{\frac{T(\tau)\lambda(0)}{T(0)\lambda(\tau)}} - 1$. For convenience, we define $a \equiv -\int_0^1 y^2 \frac{\dot{\tilde{\lambda}}^*(y)}{\tilde{\lambda}^*(0)} dy$, $b \equiv -\int_0^1 y \frac{\dot{\tilde{\lambda}}^*(y)}{\tilde{\lambda}^*(0)} dy > 0$, $c \equiv -\int_0^1 \frac{\dot{\tilde{\lambda}}^*(y)}{\tilde{\lambda}^*(0)} dy$, and $\chi_{\pm} \equiv [-b \pm \sqrt{b^2 - (a - \frac{1}{\tau})c}]/(a - \frac{1}{\tau})$. Detail analysis reveals that the conditions for $\langle W^* \rangle < 0$ can be classified into the following three scenarios: (I) $1/\tau > a$ (fast transition), then $\langle W^* \rangle < 0$ for $\chi_- < \chi < \chi_+$. (II) $1/\tau < a$, then $\langle W^* \rangle < 0$ for $\chi > \chi_+$ or $\chi < \chi_-$. (III) $1/\tau < a - \frac{b^2}{1 - \frac{\lambda(\tau)}{\lambda(0)}}$, then $\langle W^* \rangle$ is always negative and work can be always be extracted in this slowest scenario. Furthermore for given $\lambda^*(t)$, there is a

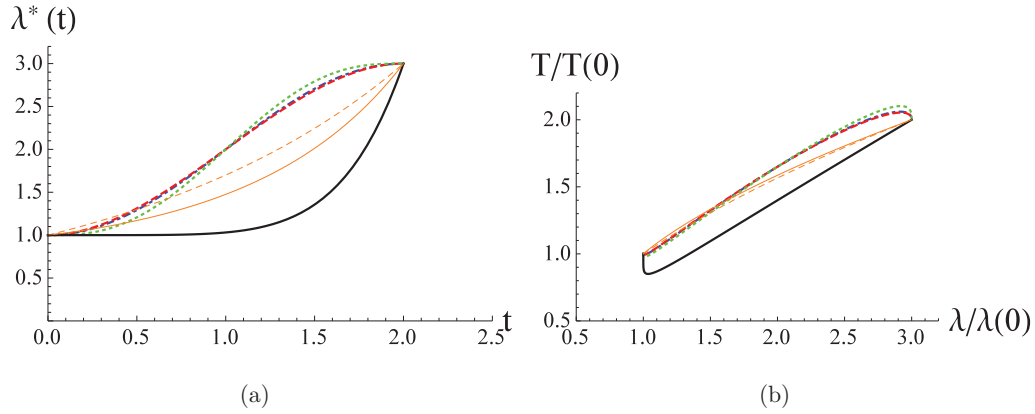


FIG. 7. (a) Several possible mdieq protocols for $\lambda^*(t)$ in the overdamped limit. Protocols: (i) blue dot-dashed curve, (ii) red dashed curve, (iii) green dotted curve and, and (iv) $\mu = 6$, thick black solid curve. The cases of underdamped mdieq protocols are also shown for comparison for $\alpha = 10$ (orange thin solid curve), $\alpha = 1$ (orange thin dashed curve). (b) The mdieq protocols shown in the λ - T plane for the cases in (a).

negative minimum $\langle W^* \rangle$ at some value of $\chi = \chi_{\min}$ under the fast scenario (I), which can be derived analytical to be

$$\chi_{\min} = \frac{b\tau}{1 - a\tau} \Rightarrow \left(\frac{T(\tau) \lambda(0)}{T(0) \lambda(\tau)} \right)_{\min} = \left(\frac{1 + (b - a)\tau}{1 - a\tau} \right)^2, \quad (61)$$

$$\langle W^* \rangle_{\min} = -\frac{T(0)}{2} \left(\frac{b^2\tau}{1 - a\tau} + c \right). \quad (62)$$

Figure 8(a) shows $\langle W^* \rangle$ as a function of $\frac{T(\tau)}{T(0)}$ with $\frac{\lambda(\tau)}{\lambda(0)} = \frac{1}{3}$ in the fast scenario (I) for various mdieq protocols in Fig. 7. The

corresponding mean heat is given by $\langle Q^* \rangle = \Delta T - \Delta \Phi^* + 2\Delta U_1^*$ and is plotted as a function of $\frac{T(\tau)}{T(0)}$ in Fig. 8(b). Since $\langle W^* \rangle$ has a minimum, $\langle Q^* \rangle$ has a maximum also, but is located at large values of $\frac{T(\tau)}{T(0)}$ beyond the range shown in the figure.

The power can be directly computed from $P^* = -\langle W^* \rangle / \tau$ and also displays a maximum as a function of τ as shown in Figs. 8(c) and 8(d), with the maximal power and τ_{\max} derived to be

$$\tau_{\max} = \frac{2\chi^2}{a\chi^2 + 2b\chi + c}, \quad P^*_{\max} = \frac{(a\chi^2 + 2b\chi + c)^2}{8\chi^2} T(0). \quad (63)$$

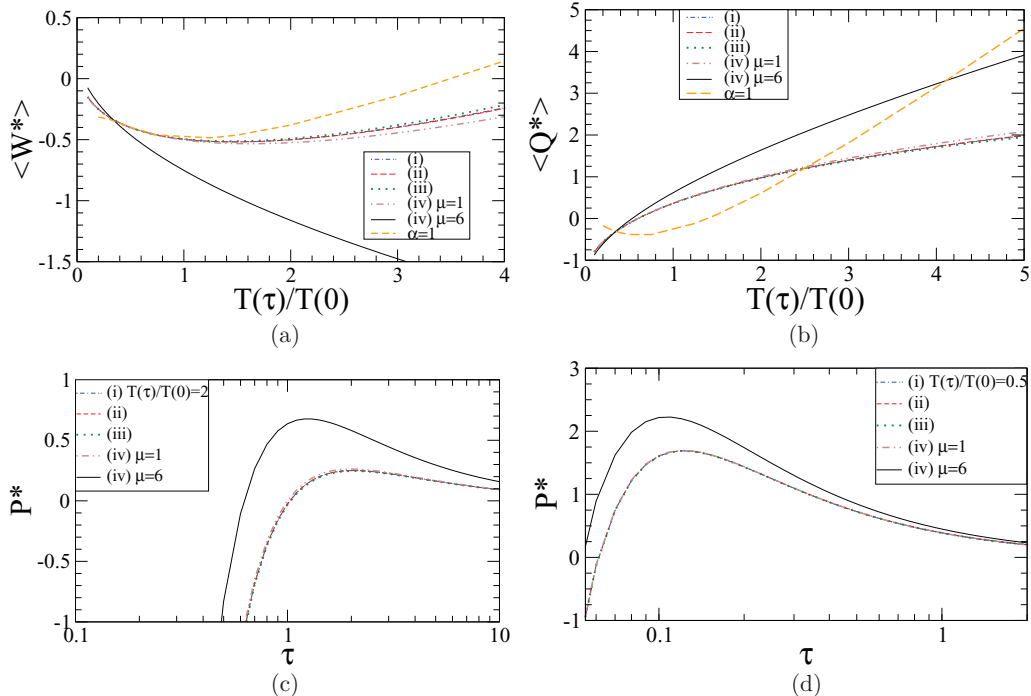


FIG. 8. mdieq energetics [in unit of $T(0)$] in the overdamped limit for $\frac{\lambda(\tau)}{\lambda(0)} = \frac{1}{3}$ (expansion). (a) Mean work, $\langle W^* \rangle$ for the mdieq transition in the overdamped limit for the protocols (i)–(iv) with $\tau = 2$ [fast scenario (I)]. The case of underdamped mdieq protocol is also shown for comparison for $\alpha = 1$ (orange thin dashed curve). (b) Mean heat, $\langle Q^* \rangle$ for the cases in (a). (c) The mdieq mean power extracted as a function of τ for the cases in (a) for $\frac{T(\tau)}{T(0)} = 2$. (d) The mdieq mean power extracted as a function of τ for the cases in (a) for $\frac{T(\tau)}{T(0)} = 0.5$.

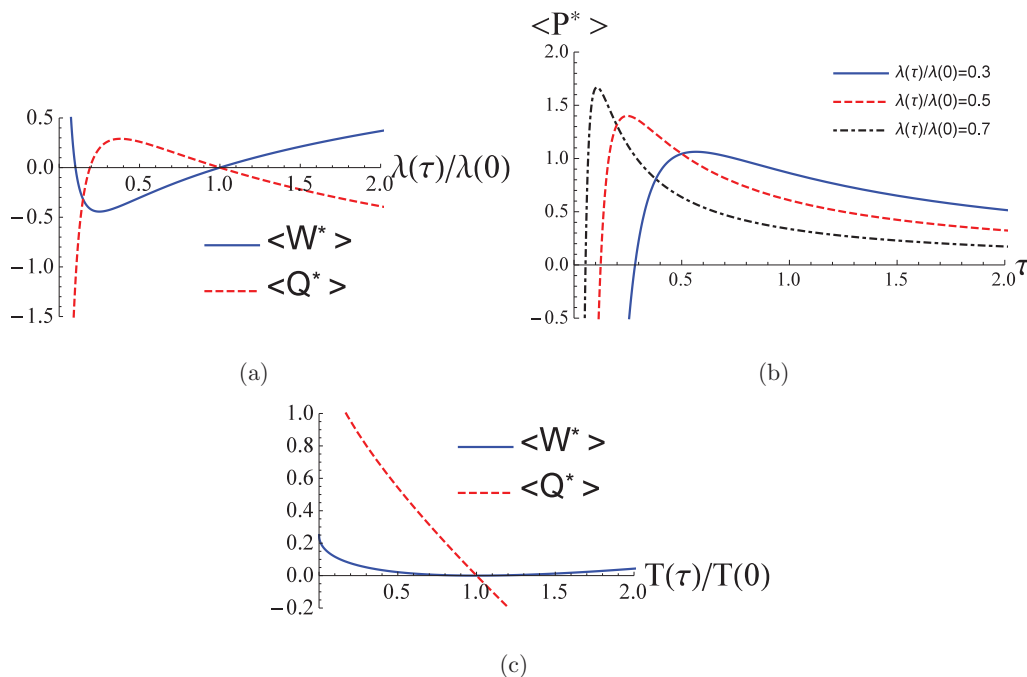


FIG. 9. mdieq energetics [in unit of $T(0)$] in the overdamped limit for the isothermal and isochoric cases. (a) Mean work and heat as a function of $\frac{\lambda(\tau)}{\lambda(0)}$ for mdieq isothermal process with $\tau = 2$. (b) The isothermal mdieq mean power extracted as a function of τ for various values of $\frac{\lambda(\tau)}{\lambda(0)}$. (c) Mean work and heat as a function of $\frac{T(\tau)}{T(0)}$ for mdieq isochoric process with $\tau = 2$.

For isothermal processes, the mdieq mean heat and work in the overdamped limit can be simplified to

$$\langle W^* \rangle = \frac{T(0)}{2} \left[\ln \frac{\lambda(\tau)}{\lambda(0)} + \frac{1}{\tau} \left(1 - \sqrt{\frac{\lambda(0)}{\lambda(\tau)}} \right)^2 \right], \quad (64)$$

$$\langle Q^* \rangle = -T(0) \left[\frac{1}{2} \ln \frac{\lambda(\tau)}{\lambda(0)} + \frac{1}{\tau} \left(1 - \sqrt{\frac{\lambda(0)}{\lambda(\tau)}} \right)^2 \right]. \quad (65)$$

Figure 9(a) shows the mean work and heat as a function of compression ratio $\frac{\lambda(\tau)}{\lambda(0)}$ for the isothermal case. Work extraction ($\langle W^* \rangle < 0$) is possible only for the case of expansion ($\frac{\lambda(\tau)}{\lambda(0)} < 1$), and there is an optimal expansion ratio at which maximal work can be extracted, which can be calculated to be

$$\left(\frac{\lambda(\tau)}{\lambda(0)} \right)_{\min} = \frac{1}{4\tau^2} (\sqrt{1+4\tau} - 1)^2, \quad (66)$$

$$\langle W^* \rangle_{\min} = T \left[\ln \left(\frac{\sqrt{1+4\tau} - 1}{2\tau} \right) + \frac{1}{\tau} \left(\frac{2\tau}{\sqrt{1+4\tau} - 1} - 1 \right)^2 \right]. \quad (67)$$

The power $P^* = -\langle W^* \rangle / \tau$ in this case also displays a maximum as a function of τ if $\lambda(\tau) < \lambda(0)$, as shown in Fig. 9(b), with the maximal power and τ_{\max} derived to be

$$\tau_{\max} = 2 \frac{\left(\sqrt{\frac{\lambda(0)}{\lambda(\tau)}} - 1 \right)^2}{\ln \frac{\lambda(0)}{\lambda(\tau)}}, \quad P_{\max}^* = \frac{T}{8} \left(\frac{\ln \frac{\lambda(0)}{\lambda(\tau)}}{\sqrt{\frac{\lambda(0)}{\lambda(\tau)}} - 1} \right)^2. \quad (68)$$

Finally, for isochoric processes ($\dot{\lambda} = 0$), the mean heat and work in the overdamped limit can be calculated to give

$$\langle W^* \rangle = \frac{T(0)}{2\tau} \left(\sqrt{\frac{T(\tau)}{T(0)}} - 1 \right)^2, \quad (69)$$

$$\langle Q^* \rangle = -T(0) \left[\frac{T(\tau)}{T(0)} - 1 - \frac{1}{\tau} \left(\sqrt{\frac{T(\tau)}{T(0)}} - 1 \right)^2 \right]. \quad (70)$$

$\langle W^* \rangle$ is always non-negative and no work can be extracted in this case. Figure 9(c) shows the mean work and heat as a function of the heating ratio $\frac{T(\tau)}{T(0)}$ for the isochoric case.

IV. SUMMARY AND OUTLOOK

We have theoretically derived the ieq protocols with minimal dissipation for a Brownian particle under both time-dependent temperature and potential parameter variations. Remarkably, under the minimal dissipation condition, the time-reversal symmetry between the forward and backward processes is restored. It is worth noting that for the general ieq process, the zero entropy change protocol only requires the entropy to be the same for the initial and final state (which is less restrictive), and the path may not be isentropic. However, under the minimal dissipation condition, the zero entropy change endpoint boundary condition will enforce the mdieq path to be isentropic at all times during the transition. Such a result of mdieq being isentropic can be viewed as the generalization of the quasistatic case of zero (minimal) dissipation with a reversible (constant entropy) path. Explicit formulas of mdieq protocols for the cases of fixed temperature, fixed stiffness, and isentropic condition are derived, thus providing

TABLE I. Table summarizing the results or formulas for the mdieq protocols for the underdamped and overdamped ($\alpha \rightarrow 0$) case. The expressions for the corresponding mean work for various processes are also listed in the square bracket by the equation number in the text. For the isochoric case, the first and second equation numbers correspond to the underdamped and overdamped cases, respectively.

Process	mdieq protocol; [$\langle W^* \rangle$]	
	underdamped	overdamped
general ($\dot{T}, \dot{\lambda} \neq 0$)	solution of (22) and (23); [(27)]	$\frac{\Lambda^*(t)}{T^*(t)} = \frac{\Lambda(0)}{T(0)} \frac{1}{[1 + (\sqrt{\frac{\beta(0)\Lambda(0)}{\beta(t)\Lambda(t)} - 1}) \frac{t}{\tau}]^2}$; [(60)]
isothermal ($\dot{T} = 0$)	$\text{sh}^{-1} \sqrt{\alpha \Lambda^*} = \sqrt{1 + \frac{1}{\alpha \Lambda^*}} + c_1 - c_2 \frac{t}{\tau}$; [(43)]	$\Lambda^*(t) = \frac{\Lambda(0)}{[1 + (\sqrt{\frac{\Lambda(0)}{\Lambda(t)} - 1}) \frac{t}{\tau}]^2}$; [(64)]
isochoric ($\dot{\lambda} = 0$)		$\frac{T^*(t)}{T(0)} = [1 + (\sqrt{\frac{T(t)}{T(0)} - 1}) \frac{t}{\tau}]^2$; [(37), (69)]
isentropic ($\lambda \propto T^2$)		$\frac{T^*(t)}{T(0)} = \frac{1}{[1 - (1 - \sqrt{\frac{T(0)}{T(t)}}) \frac{t}{\tau}]^2}$; [(47)]

theoretical insights that allow the construction of desirable ieq paths with low dissipation. All the analytic formulas are summarized in Table I. With the mdieq temperature and potential protocols as building blocks, one can conveniently construct a mdieq engine cycle with the desired properties and low dissipation. The performance and associated energetics of these mdieq cycles and other general ieq cycles are under investigation and will be reported in future publications.

Furthermore, although the ieq of the isothermal process has already been implemented [7,25,26] in colloid experiments, realizing ieq protocols involving heating and cooling for underdamped systems remains challenging. Thus, in this paper, we also derive analytic results for the mdieq in the overdamped limit (see Table I for summarizing the main results). Remarkably, it is shown that there is a family of infinitely many protocols to choose to achieve mdieq in the overdamped limit. This can provide useful guidelines and great flexibility

for the choice of appropriate protocols for the experimental realization of the mdieq transitions in overdamped systems.

ACKNOWLEDGMENTS

This work has been supported by the Ministry of Science and Technology of Taiwan under Grants No. 110-2112-M-008-026-MY3 (P.-Y.L.) and No. 110-2112-M-008-006 (Y.J.), and NCTS of Taiwan.

APPENDIX A: SUMMARY OF THE IEQ TRANSITION UNDER $\lambda(t)$ AND $\beta(t)$

In order to achieve instantaneous equilibrium (ieq) under the ramp potential $U_0(x, \lambda(t))$, a position and momentum dependent auxiliary potential $U_1(x, p, t)$ is introduced in such a way that the particle experiences a total Hamiltonian

$$H = H_0(x, p, t) + U_1(x, p, t) = \frac{p^2}{2m} + U_0(x, \lambda(t)) + U_1(x, p, t), \quad (\text{A1})$$

and the underdamped Brownian particle will be at ieq that follows the Boltzmann distribution:

$$\rho_{\text{ieq}}(x, p, t) = e^{\beta(t)(F(\lambda, \beta) - H_0(x, p, \lambda(t)))}, \quad (\text{A2})$$

where $F(\lambda, \beta) = -\frac{1}{\beta(t)} \ln \int dp \int dx e^{-\beta(t)H_0(x, p, \lambda(t))}$ is the free energy of the ramp system at ieq for some instantaneous value of λ and β during the transition process. U_1 can be determined for a given ramp potential $U_0(x, \lambda(t))$ with the protocols $\lambda(t)$ and $\beta(t)$ with the requirement that $\rho_{\text{ieq}}(x, t)$ must satisfy the Kramers equation

$$\frac{\partial \rho_{\text{ieq}}}{\partial t} = -\frac{\partial}{\partial x} \left[\rho_{\text{ieq}} \left(\frac{p}{m} + \frac{\partial U_1}{\partial p} \right) \right] + \frac{\partial}{\partial p} \left[\rho_{\text{ieq}} \left(\frac{\partial U_0}{\partial x} + \frac{\partial U_1}{\partial x} + \frac{\gamma p}{m} + \gamma \frac{\partial U_1}{\partial p} + \frac{\gamma}{\beta(t) \rho_{\text{ieq}}} \frac{\partial \rho_{\text{ieq}}}{\partial p} \right) \right], \quad (\text{A3})$$

resulting in a linear PDE for U_1 :

$$\frac{\gamma}{\beta} \frac{\partial^2 U_1}{\partial p^2} + \left(\frac{\partial U_0}{\partial x} - \frac{\gamma p}{m} \right) \frac{\partial U_1}{\partial p} - \frac{p}{m} \frac{\partial U_1}{\partial x} = \frac{\dot{\beta}}{\beta} (F - H_0) + \dot{\beta} \frac{\partial F}{\partial \beta} + \left(\frac{\partial F}{\partial \lambda} - \frac{\partial U_0}{\partial \lambda} \right) \dot{\lambda}. \quad (\text{A4})$$

The linear dependence of $\dot{\lambda}$ and $\dot{\beta}$ in the RHS of (A4) implies that U_1 is of the form given by (3). Since (A4) is linear in U_1 for general $U_0(x, \lambda(t))$, one can employ the power series expansion method to solve for U_1 . For the case of $U_0(x, \lambda) = \frac{1}{2} \lambda x^n$, U_1 was derived [27] to be

$$U_1(x, p, t) = \frac{\tau_m \dot{\lambda}(t)}{n \lambda(t)} H_0(x, p - \gamma x, \lambda(t)) + \frac{\tau_m \dot{\beta}(t)}{\beta(t)} \left[\frac{1}{2} H_0(x, p, \lambda(t)) + \frac{1}{n} H_0(x, p - \gamma x, \lambda(t)) \right], \quad (\text{A5})$$

where $\tau_m \equiv m/\gamma$ is the inertia memory time of the underdamped particle. The underdamped particle experiences the total potential

$$U_{\text{ieq}} = \frac{1}{2} \lambda(t) x^n + U_1(x, p, t) \quad (\text{A6})$$

and follows the ieq Boltzmann distribution with the instantaneous free energy, given respectively by

$$\rho_{\text{ieq}}(x, p, t) = e^{\beta(t)[F(\lambda(t), \beta(t)) - \frac{p^2}{2m} - \frac{\lambda(t)}{2}x^n]}, \tag{A7}$$

$$\beta(t)F(\lambda(t), \beta(t)) = \ln \left[\frac{n}{2\Gamma(\frac{1}{n})} \left(\frac{\beta(t)\lambda(t)}{2} \right)^{\frac{1}{n}} \sqrt{\frac{\beta(t)}{2\pi m}} \right] \tag{A8}$$

$$= \frac{1}{n} \ln \lambda(t) + \left(\frac{1}{2} + \frac{1}{n} \right) \ln \beta(t) + \text{constant}, \tag{A9}$$

where $\Gamma(x)$ is the Gamma function. Denote the (time-dependent) ensemble average at ieq by $\langle \dots \rangle \equiv \int dx \int dp \dots \rho_{\text{ieq}}(x, p, t)$, direct calculations give

$$\langle p^2(t) \rangle = \frac{m}{\beta(t)}; \quad \langle x^n(t) \rangle = \frac{2}{n\beta(t)\lambda(t)}; \quad \langle x^2(t) \rangle = \left(\frac{2}{\beta(t)\lambda(t)} \right)^{\frac{2}{n}} \frac{\Gamma(\frac{3}{n})}{\Gamma(\frac{1}{n})}, \tag{A10}$$

which in dimensionless form is (8) in the main text.

The infinitesimal work (dW) for the ieq trajectory from time t to $t + dt$ can be calculated directly from (5) and (6) to give

$$\beta_0 dW = \beta_0 \frac{\partial(U_0 + U_1)}{\partial t} dt \tag{A11}$$

$$= \left\{ \left[\frac{1}{2} \left(1 + \frac{\alpha}{n} v(t) + \frac{\alpha}{2} \frac{\dot{\beta}(t)}{\beta(t)} \right) \dot{\Lambda}(t) + \frac{\alpha}{2} \Lambda(t) \left[\frac{\dot{v}(t)}{n} + \frac{1}{2} \frac{d}{dt} \left(\frac{\dot{\beta}(t)}{\beta(t)} \right) \right] \right] x^n \right. \tag{A12}$$

$$\left. + \frac{\dot{v}(t)}{2n} (\alpha p - x)^2 + \frac{1}{4} \frac{d}{dt} \left(\frac{\dot{\beta}(t)}{\beta(t)} \right) (\alpha p)^2 \right\} dt.$$

The mean work in the ieq process can then be computed theoretically by taking the ensemble average of (A12) and using (A10) to give

$$\langle W \rangle = \int_0^\tau dt \left\langle \frac{\partial(U_0 + U_1)}{\partial t} \right\rangle \equiv \Delta\Phi + W_{\text{diss}} \tag{A13}$$

$$= \frac{1}{n} \int_0^\tau \frac{\dot{\Lambda}(t)}{\beta(t)\Lambda(t)} dt + W_{\text{diss}}, \tag{A14}$$

where the mean dissipated work in the ieq process is given by $W_{\text{diss}} = \int_0^\tau dt \langle \frac{\partial U_1}{\partial t} \rangle$. The mean dissipated work in the ieq process $W_{\text{diss}} = \int_0^\tau dt \langle \frac{\partial U_1}{\partial t} \rangle$ is given by

$$W_{\text{diss}} = \int_0^\tau dt \frac{\alpha}{\beta(t)} \left[\frac{1}{n} \left(\frac{v(t)}{n} + \frac{\dot{\beta}(t)}{2\beta(t)} \right) \frac{\dot{\Lambda}(t)}{\Lambda(t)} + \left(\frac{1}{2} + \frac{1}{n} \right) \left(\frac{\dot{v}(t)}{n} + \frac{1}{2} \frac{d}{dt} \left(\frac{\dot{\beta}(t)}{\beta(t)} \right) \right) + \frac{\beta \dot{v}}{2\alpha n \beta_0} \frac{\Gamma(\frac{3}{n})}{\Gamma(\frac{1}{n})} \left(\frac{2\beta_0}{\beta(t)\Lambda(t)} \right)^{\frac{2}{n}} \right] \tag{A15}$$

$$\equiv \Delta U_1 + \int_0^\tau \mathcal{L}_n(\Lambda(t), \dot{\Lambda}(t), \beta(t), \dot{\beta}(t)) dt, \quad \text{where}$$

$$\mathcal{L}_n \equiv \frac{\alpha}{\beta} \left(\frac{v}{n} + \frac{\dot{\beta}}{2\beta} \right)^2 + \frac{1}{n^2 \beta_0} \frac{\Gamma(\frac{3}{n})}{\Gamma(\frac{1}{n})} \left(\frac{2\beta_0}{\beta\Lambda} \right)^{\frac{2}{n}} v^2. \tag{A16}$$

\mathcal{L}_n can be put in terms of a metric tensor \mathbf{g} (from which a thermodynamic distance [40] can be defined in the parameter space),

$$\mathcal{L}_n = \begin{pmatrix} \dot{\Lambda} & \dot{\beta} \\ \dot{\Lambda} & \dot{\beta} \end{pmatrix} \mathbf{g} \begin{pmatrix} \dot{\Lambda} \\ \dot{\beta} \end{pmatrix}, \quad \text{where} \tag{A17}$$

$$\mathbf{g} \equiv \frac{1}{n^2 \beta} \begin{pmatrix} \alpha + \frac{D_n}{\Lambda^{2/n}} & (1 + \frac{n}{2})\alpha + \frac{D_n}{\Lambda^{2/n}} \\ (1 + \frac{n}{2})\alpha + \frac{D_n}{\Lambda^{2/n}} & (1 + \frac{n}{2})^2 \alpha + \frac{D_n}{\Lambda^{2/n}} \end{pmatrix}, \quad D_n \equiv 2 \left(\frac{\beta}{2\beta_0} \right)^{1 - \frac{2}{n}} \frac{\Gamma(\frac{3}{n})}{\Gamma(\frac{1}{n})}. \tag{A18}$$

APPENDIX B: PROOF OF EQ. (26)

For harmonic potential, from (10) (with $n = 2$), we have

$$\langle U_1 \rangle = \frac{\dot{\beta}}{\beta^2} \left(\alpha + \frac{1}{4\Lambda} \right) + \frac{\dot{\Lambda}}{2\beta\Lambda} \left(\alpha + \frac{1}{2\Lambda} \right). \tag{B1}$$

Under the mdieq protocol Λ^* and β^* satisfy (22) and (23) which can be rewritten explicitly in terms of β , Λ , and their derivatives,

$$\frac{2\ddot{\beta}}{\beta}\left(\alpha + \frac{1}{2\Lambda}\right) + \frac{\ddot{\Lambda}}{\Lambda}\left(\alpha + \frac{1}{\Lambda}\right) - \frac{\dot{\Lambda}^2}{\Lambda^2}\left(\alpha + \frac{3}{2\Lambda}\right) - \frac{4\dot{\beta}^2}{\beta^2}\left(\alpha + \frac{3}{8\Lambda}\right) - \frac{\dot{\beta}\dot{\Lambda}}{\beta\Lambda^2} = 0, \tag{B2}$$

$$\frac{4\dot{\beta}}{\beta}\left(\alpha + \frac{1}{4\Lambda}\right) + \frac{2\dot{\Lambda}}{\Lambda}\left(\alpha + \frac{1}{2\Lambda}\right) - \frac{3\dot{\Lambda}^2}{2\Lambda^2}\left(\alpha + \frac{1}{\Lambda}\right) - \frac{6\dot{\beta}^2}{\beta^2}\left(\alpha + \frac{1}{4\Lambda}\right) - \frac{\dot{\beta}\dot{\Lambda}}{\beta\Lambda^2} = 0. \tag{B3}$$

Then expanding \mathcal{L}_2 in (21) with the mdieq solution

$$\int_0^\tau \mathcal{L}_2^* dt = \int_0^\tau dt \left\{ \frac{\dot{\beta}^{*2}}{\beta^{*3}}\left(\alpha + \frac{1}{4\Lambda^*}\right) + \frac{\dot{\beta}^*\dot{\Lambda}^*}{\beta^{*2}\Lambda^*}\left(\alpha + \frac{1}{2\Lambda^*}\right) + \frac{1}{4}\frac{\dot{\Lambda}^{*2}}{\beta^*\Lambda^{*2}}\left(\alpha + \frac{1}{\Lambda^*}\right) \right\}. \tag{B4}$$

Integrating by parts the first term and invoking (B3), we have

$$\int_0^\tau \frac{\dot{\beta}^{*2}}{\beta^{*3}}\left(\alpha + \frac{1}{4\Lambda^*}\right) dt = -\frac{2\dot{\beta}^*}{\beta^{*2}}\left(\alpha + \frac{1}{4\Lambda^*}\right) \Big|_0^\tau + \int_0^\tau dt \left\{ \frac{3}{4}\frac{\dot{\Lambda}^{*2}}{\beta^*\Lambda^{*2}}\left(\alpha + \frac{1}{\Lambda^*}\right) - \frac{\ddot{\Lambda}^*}{\beta^*\Lambda^*}\left(\alpha + \frac{1}{2\Lambda^*}\right) \right\}. \tag{B5}$$

Substituting the above back to (B4) and then invoking (B1), we have

$$\int_0^\tau \mathcal{L}_2^* dt = -\frac{2\dot{\beta}^*}{\beta^{*2}}\left(\alpha + \frac{1}{4\Lambda^*}\right) \Big|_0^\tau - \frac{\dot{\Lambda}^{*2}}{\beta^*\Lambda^{*2}}\left(\alpha + \frac{1}{\Lambda^*}\right) \Big|_0^\tau \tag{B6}$$

$$= -2(\langle U_1^*(\tau) \rangle - \langle U_1^*(0) \rangle) = -2\Delta U_1^*. \tag{B7}$$

Notice that only (B3) [but not (B2)] is needed in the proof, and hence (26) holds for $\dot{\beta} \neq 0$.

APPENDIX C: RESTORATION OF TIME-REVERSAL SYMMETRY IN THE BACKWARD MDIEQ PROTOCOLS

Consider a forward process of $(\lambda(0), \beta(0)) \rightarrow (\lambda(\tau), \beta(\tau))$ and $\Lambda(t)$ is the dimensionless protocol of $\lambda(t)$ scaled with some fixed stiffness, say $\Lambda(t) \equiv \lambda(t)/\lambda_0$, the mdieq protocols obey (B2) and (B3). The backward path connects $(\lambda(\tau), \beta(\tau)) \rightarrow (\lambda(0), \beta(0))$ with some protocols $\lambda_r(t)$ and $\beta_r(t)$, i.e., $\beta_r(0) = \beta(\tau)$, $\beta_r(\tau) = \beta(0)$, $\lambda_r(0) = \lambda(\tau)$, $\lambda_r(\tau) = \lambda(0)$. The mdieq protocols for the backward process are also governed by (B2) and (B3). With $t \rightarrow \tau - t$, (B2) and (B3) for the mdieq backward protocols read

$$\begin{aligned} &\frac{2\dot{\beta}_r^*(\tau - t)}{\beta_r^*(\tau - t)}\left(\alpha + \frac{\lambda_0}{2\lambda_r^*(\tau - t)}\right) + \frac{\dot{\lambda}_r^*(\tau - t)}{\lambda_r^*(\tau - t)}\left(\alpha + \frac{\lambda_0}{\lambda_r^*(\tau - t)}\right) - \frac{\dot{\lambda}_r^{*2}(\tau - t)}{\lambda_r^{*2}(\tau - t)}\left(\alpha + \frac{\lambda_0}{2\lambda_r^*(\tau - t)}\right) \\ &- \frac{4\dot{\beta}_r^{*2}(\tau - t)}{\beta_r^{*2}(\tau - t)}\left(\alpha + \frac{3\lambda_0}{8\lambda_r^*(\tau - t)}\right) - \frac{\dot{\beta}_r^*(\tau - t)\dot{\lambda}_r^*(\tau - t)}{\beta_r^*(\tau - t)\lambda_r^{*2}(\tau - t)} = 0, \end{aligned} \tag{C1}$$

$$\begin{aligned} &\frac{4\dot{\beta}_r^*(\tau - t)}{\beta_r^*(\tau - t)}\left(\alpha + \frac{\lambda_0}{4\lambda_r^*(\tau - t)}\right) + \frac{2\dot{\lambda}_r^*(\tau - t)}{\lambda_r^*(\tau - t)}\left(\alpha + \frac{\lambda_0}{2\lambda_r^*(\tau - t)}\right) - \frac{3\dot{\lambda}_r^{*2}(\tau - t)}{2\lambda_r^{*2}(\tau - t)}\left(\alpha + \frac{\lambda_0}{\lambda_r^*(\tau - t)}\right) \\ &- \frac{6\dot{\beta}_r^{*2}(\tau - t)}{\beta_r^{*2}(\tau - t)}\left(\alpha + \frac{\lambda_0}{4\lambda_r^*(\tau - t)}\right) - \frac{\dot{\beta}_r^*(\tau - t)\dot{\lambda}_r^*(\tau - t)}{\beta_r^*(\tau - t)\lambda_r^{*2}(\tau - t)} = 0, \end{aligned} \tag{C2}$$

which are the same equations governing the mdieq protocols, $\lambda^*(t)$ and $\beta^*(t)$, of the forward process. Thus we have the time-reversal symmetric relation for the mdieq protocols of the forward and backward processes, namely,

$$\lambda_r^*(\tau - t) = \lambda^*(t), \quad \beta_r^*(\tau - t) = \beta^*(t). \tag{C3}$$

It is easy to see that the proper endpoints B.C.s for λ_r^* and β_r^* also hold. Furthermore, since

$$\int_0^\tau \mathcal{L}_2(\lambda^*(\tau - t), \dot{\lambda}^*(\tau - t), \beta^*(\tau - t), \dot{\beta}^*(\tau - t)) dt = \int_0^\tau \mathcal{L}_2(\lambda^*(t), \dot{\lambda}^*(t), \beta^*(t), \dot{\beta}^*(t)) dt. \tag{C4}$$

Using (B1) to compute the ΔU_{1r}^* of the mdieq of the backward process, we have

$$\Delta U_{1r}^* = \frac{\dot{\beta}_r^*(\tau)}{\beta(0)^2}\left(\alpha + \frac{\lambda_0}{4\lambda(0)}\right) - \frac{\dot{\beta}_r^*(0)}{\beta(\tau)^2}\left(\alpha + \frac{\lambda_0}{4\lambda(\tau)}\right) \tag{C5}$$

$$+ \frac{\dot{\lambda}_r^*(\tau)}{2\beta(0)\lambda(0)}\left(\alpha + \frac{\lambda_0}{2\lambda(0)}\right) - \frac{\dot{\lambda}_r^*(0)}{2\beta(\tau)\lambda(\tau)}\left(\alpha + \frac{\lambda_0}{2\lambda(\tau)}\right) = \Delta U_1^*, \tag{C6}$$

where the last equality follows from (C3). Since $W_{\text{diss}}^* = \Delta U_1^* + \int_0^\tau \mathcal{L}_2^* dt$, hence the minimized dissipative works for the forward and backward mdieq processes are the same,

$$W_{\text{diss}r}^* = W_{\text{diss}}^*. \quad (\text{C7})$$

One can similarly compute

$$\Delta \Phi_r^* = \frac{1}{2} \int_0^\tau \frac{\dot{\lambda}_r^*(t)}{\beta_r^*(t)\lambda_r^*(t)} dt = -\frac{1}{2} \int_0^\tau \frac{\dot{\lambda}^*(\tau-t)}{\beta^*(\tau-t)\lambda^*(\tau-t)} dt = -\Delta \Phi^*. \quad (\text{C8})$$

Hence we derive the work relation between the forward and reverse mdieq

$$\langle W^* \rangle = \langle W_r^* \rangle + 2\Delta \Phi^*, \quad (\text{C9})$$

which is a special case of the work relation for the general ieq of the forward and reverse process [27].

-
- [1] C. Jarzynski, Equilibrium free-energy differences from nonequilibrium measurements: A master-equation approach, *Phys. Rev. E* **56**, 5018 (1997).
- [2] G. E. Crooks, Entropy production fluctuation theorem and the nonequilibrium work relation for free energy differences, *Phys. Rev. E* **60**, 2721 (1999).
- [3] K. Sekimoto, *Stochastic Energetics*, Lecture Notes in Physics, Vol. 799 (Springer, Berlin, Heidelberg, 2010).
- [4] U. Seifert, Stochastic thermodynamics, fluctuation theorems and molecular machines, *Rep. Prog. Phys.* **75**, 126001 (2012).
- [5] D. Carberry, J. Reid, G. Wang, E. Sevick, D. Searles, and D. Evans, Fluctuations and Irreversibility: An Experimental Demonstration of a Second-Law-Like Theorem Using a Colloidal Particle Held in an Optical Trap, *Phys. Rev. Lett.* **92**, 140601 (2004).
- [6] J. A. C. Albay, G. Paneru, H. Kyu Pak, and Y. Jun, Optical tweezers as a mathematically driven spatio-temporal potential generator, *Opt. Express* **26**, 29906 (2018).
- [7] J. A. C. Albay, P.-Y. Lai, and Y. Jun, Realization of finite-rate isothermal compression and expansion using optical feedback trap, *Appl. Phys. Lett.* **116**, 103706 (2020).
- [8] K.-H. Chiang, C.-L. Lee, P.-Y. Lai, and Y.-F. Chen, Entropy production and irreversibility of dissipative trajectories in electric circuits, *Phys. Rev. E* **95**, 012158 (2017).
- [9] K.-H. Chiang, C.-L. Lee, P.-Y. Lai, and Y.-F. Chen, Electrical autonomous brownian gyrator, *Phys. Rev. E* **96**, 032123 (2017).
- [10] N. Freitas, Jean-C. Delvenne, and M. Esposito, Stochastic and Quantum Thermodynamics of Driven RLC Networks, *Phys. Rev. X* **10**, 031005 (2020).
- [11] V. Blickle and C. Bechinger, Realization of a micrometre-sized stochastic heat engine, *Nat. Phys.* **8**, 143 (2012).
- [12] I. A. Martínez, È. Roldán, L. Dinis, D. Petrov, J. M. R. Parrondo, and R. A. Rica, Brownian Carnot engine, *Nat. Phys.* **12**, 67 (2016).
- [13] J. A. C. Albay, Z.-Y. Zhou, C.-H. Chang, and Y. Jun, Shift a laser beam back and forth to exchange heat and work in thermodynamics, *Sci. Rep.* **11**, 4394 (2021).
- [14] D. Collin, F. Ritort, C. Jarzynski, S. B. Smith, I. Tinoco, and C. Bustamante, Verification of the Crooks fluctuation theorem and recovery of RNA folding free energies, *Nature* **437**, 231 (2005).
- [15] J. Liphardt, S. Dumont, S. B. Smith, I. Tinoco, and C. Bustamante, Equilibrium information from nonequilibrium measurements in an experimental test of Jarzynski's equality, *Science* **296**, 1832 (2002).
- [16] T. B. Batalhão, A. M. Souza, L. Mazzola, R. Auccaise, R. S. Sarthour, I. S. Oliveira, J. Goold, G. De Chiara, M. Paternostro, and R. M. Serra, Experimental Reconstruction of Work Distribution and Study of Fluctuation Relations in a Closed Quantum System, *Phys. Rev. Lett.* **113**, 140601 (2014).
- [17] S. An, J. N. Zhang, M. Um, D. Lv, Y. Lu, J. Zhang, Z. Q. Yin, H. T. Quan, and K. Kim, Experimental test of the quantum Jarzynski equality with a trapped-ion system, *Nat. Phys.* **11**, 193 (2015).
- [18] I. A. Martínez, A. Petrosyan, D. Guéry-Odelin, E. Trizac, and S. Ciliberto, Engineered swift equilibration of a Brownian particle, *Nat. Phys.* **12**, 843 (2016).
- [19] M. Chupeau, J. Gladrow, A. Chepelianskii, U. F. Keyser, and E. Trizac, Optimizing Brownian escape rates by potential shaping, *Proc. Natl. Acad. Sci. U.S.A.* **117**, 1383 (2020).
- [20] C. A. Plata, D. Guéry-Odelin, E. Trizac, and A. Prados, Finite-time adiabatic processes: Derivation and speed limit, *Phys. Rev. E* **101**, 032129 (2020).
- [21] Y. Rosales-Cabara, G. Manfredi, G. Schnoering, P.-A. Hervieux, L. Mertz, and C. Genet, Optimal protocols and universal time-energy bound in brownian thermodynamics, *Phys. Rev. Research* **2**, 012012(R) (2020).
- [22] D. Guéry-Odelin, A. Ruschhaupt, A. Kiely, E. Torrontegui, S. Martínez-Garaot, and J. G. Muga, Shortcuts to adiabaticity: Concepts, methods, and applications, *Rev. Mod. Phys.* **91**, 045001 (2019).
- [23] G. Li, H. T. Quan, and Z. C. Tu, Shortcuts to isothermality and nonequilibrium work relations, *Phys. Rev. E* **96**, 012144 (2017).
- [24] G. Li and Z. C. Tu, Stochastic thermodynamics with odd controlling parameters, *Phys. Rev. E* **100**, 012127 (2019).
- [25] J. A. C. Albay, S. R. Wulaningrum, C. Kwon, P.-Y. Lai, and Y. Jun, Thermodynamic cost of a shortcuts-to-isothermal transport of a Brownian particle, *Phys. Rev. Research* **1**, 033122 (2019).
- [26] J. A. C. Albay, C. Kwon, P.-Y. Lai, and Y. Jun, Work relation in instantaneous-equilibrium transition of forward and reverse processes, *New J. Phys.* **22**, 123049 (2020).
- [27] Y. Jun and P.-Y. Lai, Instantaneous equilibrium transition for brownian systems under time-dependent temperature and potential variations: Reversibility, heat and work relations, and fast isentropic process, *Phys. Rev. Research* **3**, 033130 (2021).
- [28] E. Aurell, C. Mejía-Monasterio, and P. Muratore-Ginanneschi, Boundary layers in stochastic thermodynamics, *Phys. Rev. E* **85**, 020103(R) (2012).

- [29] K. Nakamura, J. Matrasulov, and Y. Izumida, Fast-forward approach to stochastic heat engine, *Phys. Rev. E* **102**, 012129 (2020).
- [30] A. Prados, Optimizing the relaxation route with optimal control, *Phys. Rev. Research* **3**, 023128 (2021).
- [31] C. A. Plata, A. Prados, E. Trizac, and D. Guéry-Odelin, Taming the Time Evolution in Overdamped Systems: Shortcuts Elaborated from Fast-Forward and Time-Reversed Protocols, *Phys. Rev. Lett.* **127**, 190605 (2021).
- [32] T. Schmiedl and U. Seifert, Optimal Finite-Time Processes In Stochastic Thermodynamics, *Phys. Rev. Lett.* **98**, 108301 (2007).
- [33] E. Aurell, C. Mejía-Monasterio, and P. Muratore-Ginanneschi, Optimal Protocols and Optimal Transport in Stochastic Thermodynamics, *Phys. Rev. Lett.* **106**, 250601 (2011).
- [34] Y. Zhang, Work needed to drive a thermodynamic system between two distributions, *Europhys. Lett.* **128**, 30002 (2019).
- [35] A. G. Frim and M. R. DeWeese, Optimal finite-time Brownian Carnot engine, *Phys. Rev. E* **105**, L052103 (2022).
- [36] G. Li, J.-F. Chen, C. P. Sun, and H. Dong, Geodesic path for the minimal energy cost in shortcuts to isothermality, [arXiv:2110.09137](https://arxiv.org/abs/2110.09137).
- [37] Z.-C. Tu, Abstract models for heat engines, *Front. Phys.* **16**, 33202 (2021).
- [38] For general n , in the $\alpha \rightarrow 0$ limit, the Euler-Lagrange equation reads $\dot{v} = \frac{v^2}{n}$ and the mdieq protocol is $\beta^*(t)\lambda^*(t) = \frac{\beta(0)\lambda(0)}{[1+(1+\frac{\beta(0)\lambda(0)}{\beta(\tau)\lambda(\tau)})^{\frac{1}{n}}-1]^{\frac{1}{n}}}$.
- [39] Note that $\lim_{\alpha \rightarrow 0} \sqrt{\alpha}(\sqrt{1 + \frac{1}{\alpha x}} - \sinh^{-1} \sqrt{\alpha x}) = \frac{1}{\sqrt{x}}$.
- [40] D. A. Sivak and G. E. Crooks, Thermodynamic Metrics and Optimal Paths, *Phys. Rev. Lett.* **108**, 190602 (2012).